Development of Immunostimulatory Motif-containing DNA-based Delivery System for Drugs and Antigens

（免疫刺激性モチーフを含む DNA を基盤とする
薬物および抗原デリバリーシステムの開発に関する研究）

2015

Yumiko Mizuno

Contents

Preface

The mammalian innate immune system uses pattern recognition receptors, such as Toll-like receptors (TLRs), to identify the presence of pathogens [1]. Typical structures specific to pathogenic organisms, such as lipopolysaccharide (LPS), unmethylated cytosine-phosphate-guanine (CpG) dinucleotides (CpG motifs), and double-stranded RNA, are recognized by corresponding TLRs [2, 3]. Upon activation, TLRs initiate signaling cascades that regulate the expression of a number of proteins including type I interferons and proinflammatory cytokines [4]. TLR9 is the receptor for CpG motif-containing DNA (CpG DNA). Ligation of TLR9 results in the release of tumor necrosis factor (TNF)-α, interleukin (IL)-12 and other proinflammatory cytokines, and in the stimulation of humoral and cellular immune responses [5-8]. Based on this immunostimulatory mechanism of action, substantial potential of CpG DNA as adjuvants for treatment of cancer and infectious and allergic diseases has been demonstrated in many studies [9-12].

DNA possesses some ideal characteristics as drug delivery carriers, including high biodegradability and chemical stability, and ease of large-scale production [12]. In addition, DNA has property to form complexes with some low-molecular-weight compounds and its application as a delivery carrier for anticancer agent, doxorubicin (DXR), has been investigated [13]. Furthermore, recent dramatic progress in structural DNA nanotechnology has enabled DNA to form hydrogels, which can be used as drug carriers [14].

Despite the research progress on the therapeutic application of CpG DNA and structural DNA nanotechnology, there is limited attempt to use CpG DNA as drug carriers so far and the potential of CpG DNA as drug delivery system (DDS) carriers is not clear. Therefore, in this thesis, I aimed to investigate to develop CpG DNA-based DDS to deliver drugs and antigen proteins.

In Chapter I, plasmid DNA (pDNA) was used as a CpG DNA, because it is a bacterial DNA which originally contains large numbers of CpG motifs and can be manipulated in bacteria in large quantities at a low cost. A commonly used anticancer agent, DXR, was selected as a drug to be delivered. To selectively deliver DXR to tumor tissues, DXR was intercalated to pDNA to obtain pDNA/DXR complex, and then its effect on the tumor growth was investigated in mice with hepatic metastasis.

In Chapter II, synthetic CpG motif-containing oligodeoxynucleotides (ODNs) were used as CpG DNA considering the safety in clinical application. My laboratory recently developed a novel method to prepare a ligase-free, self-gelling and injectable DNA hydrogel which consists of polypod-like structured DNA prepared using CpG motif-containing ODNs. This immunostimulatory DNA hydrogel (sDNA hydrogel) was shown to be effective as a vaccine adjuvant for cancer immunotherapy by intradermal immunization [15]. I extended these results and aimed to develop an sDNA hydrogel-based advanced antigen delivery system.

In Section 1 of Chapter II, the effectiveness of sDNA hydrogel as nasal antigen delivery carriers for allergy immunotherapy was investigated, because the potential of this sDNA hydrogel as a carrier for mucosal delivery or allergy immunotherapy has not been investigated so far. sDNA hydrogel loaded with Cryj1, a major Japanese cedar pollen allergen (Cryj1/sDNA hydrogel) was developed. Then the physicochemical properties and biological activity of the Cryj1/sDNA hydrogel were examined after

intranasal administration to mice, to evaluate the potential of the sDNA hydrogel as a nasal delivery carrier to induce immunotherapeutic effects against allergic rhinitis.

In Section 2 of Chapter II, I aimed to optimize the release profile of antigen from sDNA hydrogel to improve the usefulness of sDNA hydrogel, because sustained release of CpG DNA and antigen is expected to lead to efficient antigen specific immune response. Chitosan, a cationic polymer, was selected to stabilize sDNA hydrogel by electrostatic interaction between chitosan and DNA, and then its property on sustained release of antigen and induction of antigen specific immune response was investigated.

In this thesis, the results are presented in the following two chapters.

Chapter I

Development of anticancer drug delivery system based on immunostimulatory-motif containing plasmid DNA

I-1 Introduction

A variety of treatments has been proposed and developed to treat cancer patients, including surgery, radiation, chemotherapy and their combinations. Cancer immunotherapy is a relatively new and promising concept for the treatment of cancer, by which the host immune system is activated to destroy cancer cells. Under healthy conditions, the immune system identifies cancerous cells and destroys them in an efficient manner. This process is highly important for multi-cellular organisms, such as humans, to ensure a long life, because a number of cells can become malignant at any time. Thus, the activation of the immune system seems to be a safe and promising method to treat cancer patients. A variety of approaches has been developed for cancer immunotherapy, including the administration of tumor-related antigens, with or without various adjuvants, and the administration of activated immune cells [16-18].

Activation of innate immunity is a prerequisite for the induction of an adaptive immune response and, therefore, it plays an important role in the development of effective cancer immunotherapy. The mammalian innate immune system uses pattern recognition receptors, such as Toll-like receptors (TLRs), to identify the presence of pathogens [1]. Typical structures specific to pathogenic organisms, such as lipopolysaccharide (LPS), unmethylated CpG dinucleotides, or CpG motifs, and double-stranded RNA, are recognized by corresponding TLRs [2, 3]. Upon activation, TLRs initiate signaling cascades that regulate the expression of a number of proteins including type I interferons and proinflammatory cytokines [4]. Therefore, the use of TLR ligands has been considered to be effective in inducing an anticancer immune response.

Site-specific delivery of anticancer agents to solid tumors has been proved to be effective for successful cancer therapy. A variety of carrier systems has been developed, including PEGylated liposomes, macromolecular micelles, nanoparticles, macromolecular prodrugs and immunoconjugates [19-23]. The accumulation of these particulate and macromolecular compounds in solid tumors has been proved to be mediated by the enhanced permeability and retention (EPR) effect [24], which can be found in most, if not all, solid tumor tissues. DNA is a class of macromolecules with suitable physicochemical properties that can be used to carry anticancer agents to solid tumors. In the early 1970s, Trouet et al. reported the first use of DNA as a carrier for DXR, one of the most frequently used anticancer agents, that intercalates into DNA to form a DNA/DXR complex [13]. They used calf thymus DNA (CT DNA) as a carrier and succeeded in obtaining better therapeutic effects with such a DNA/DXR complex [25, 26]. Although this pioneer work showed the promising effects of such complexes against malignant tumors in animal models, the use of DNA as a drug carrier has received little attention since then. This is probably due to the fact that other natural and synthetic polymers with suitable properties in terms of stability, biodegradability and productivity have been found or developed and are available for the delivery of a variety of drugs, including anticancer agents.

In the last two decades, a variety of approaches has been developed to treat diseases by administering therapeutic genes. Nonviral approaches generally use plasmid DNA as a vector for a therapeutic gene and various types of plasmid DNA or its fragments have been designed and used in preclinical and clinical studies for gene therapy [27, 28]. Plasmid DNA has many advantages as a carrier molecule for anticancer agents over CT DNA used in the previous studies by Trouet et al. [25, 26]. For example, it can be manipulated in bacteria in large quantities, and the sequence can, if required, be easily modified. Plasmid DNA is a uniformly-sized polymer with no size distribution, and this is a unique property which is not true for most natural and synthetic polymers, including CT DNA. Furthermore, plasmid DNA has a unique characteristic as bacterial DNA and contains large numbers of CpG motifs [29]. Previous studies have shown that plasmid DNA is taken up by immune cells, such as macrophages and

dendritic cells (DCs), through recognition by scavenger receptor-like mechanisms, and activates the cells to release proinflammatory cytokines, such as tumor necrosis factor (TNF)-α and interleukin (IL)-12 [30-33]. Tumor tissues consist of not only cancer cells, but also stromal cells, including infiltrating immune cells. Therefore, the use of plasmid DNA as a carrier for DXR could deliver the incorporated drug to tumor tissues as well as activate the innate immune system to release proinflammatory, antitumor cytokines.

Based on these considerations, in this section I have developed CpG motif-containing plasmid DNA (CpG plasmid DNA) and DXR complexes and examined their anticancer activity in cultured cells and animal models. A plasmid DNA containing no CpG motifs (non-CpG plasmid DNA) was also prepared and used to confirm the importance of the CpG motif in plasmid DNA on the antitumor activity of the plasmid DNA/DXR complex.

I-2 Materials and Methods

Chemicals

RPMI1640 medium, phosphate buffered saline (PBS), and Hanks' balanced salt solution (HBSS) were obtained from Nissui Pharmaceutical (Tokyo, Japan). Fetal bovine serum (FBS) was obtained from MP Biomedicals (Eschwege, Germany). Opti-modified Eagle's medium (Opti-MEM) and pcDNA3.1 were obtained from Invitrogen (Carlsbad, CA). pCpG-mcs was obtained from InvivoGen (San Diego, CA). pcDNA3.1 and pCpG-mcs were used as CpG plasmid DNA and non-CpG plasmid DNA, respectively, throughout the studies described in this manuscript. DNA samples were extensively purified with Triton X-114, a nonionic detergent, to minimize the effects of contaminated LPS. Extraction of LPS from plasmid DNA was performed according to a previously published method [32]. The level of contaminated LPS was checked by a Limulus amebocyte lysate assay using the Limulus F Single Test kit (Wako Pure Chemical Industries, Ltd, Osaka, Japan). Doxorubicin hydrochloride was also obtained from Wako Pure Chemical Industries, Ltd. Transwell plates, 12 mm in diameter with a pore size of 0.4 μm, were purchased from Corning Costar (Tokyo, Japan). All other chemicals were of the highest grade available.

Cell cultures

Murine adenocarcinoma colon26 that stably expresses firefly luciferase gene (colon26/Luc) [34] and the murine macrophage-like cell line RAW264.7 were grown in RPMI1640 medium supplemented with 10% heat-inactivated FBS, 0.15% sodium bicarbonate, 100 units/ml penicillin, 1000 μg/ml streptomycin, and 2 mM l-glutamine.

Animals

Male BALB/c mice (5-week-old) were purchased from Japan SLC, Inc. (Shizuoka, Japan). Animals were maintained under conventional housing conditions. All animal experiments were approved by the Animal Experimentation Committee of the Graduate School of Pharmaceutical Sciences, Kyoto University.

Preparation of plasmid DNA/DXR

DXR in 5% dextrose solution was added to plasmid DNA (either pcDNA3.1 or pCpG-mcs) in 5% dextrose solution and incubated for 1 h at room temperature in the dark. Binding of DXR to DNA was estimated by agarose gel electrophoresis. The concentration of plasmid DNA was measured spectrophotometrically at 260 nm. The complex was used without removal of free DXR, because the

intercalation of DXR is an equilibrium process [35].

Particle size analysis

The apparent size of plasmid DNA and plasmid DNA/DXR complex was measured using a Zetasizer (ZEN3600, Malvern Instruments, Worcestershire, UK). Briefly, samples were suspended in 5% dextrose solution at a concentration of 10 μg/50 μl, and the size was measured at 25 ℃. The average diameter was determined by triplicate analyses.

Cytotoxic assay using RAW264.7 cells

The cytotoxicity of CpG plasmid DNA/DXR complex with regard to RAW264.7 cells was determined by the MTT assay. Cells (2×10^5 cells/ml, 0.5 ml/well) were seeded on 24-well culture plates and cultured for 24 h in RPMI 1640 medium. After three washes in 0.5 ml PBS, cells were incubated with CpG plasmid DNA, DXR or CpG plasmid DNA/DXR complex for 8 h. After collection of supernatant for the measurement of TNF-α secretion, cells were incubated with 150 μl 0.5 mg/ml MTT (Sigma, St. Louis, MO, USA) in HBSS for at least 4 h at 37 °C. Then, 150 μl 10% (w/v) sodium dodecyl sulfate (Wako Pure Chemical Industries, Ltd) was added to each well, followed by an overnight incubation. Plates were then read on a microplate reader at 570 nm.

Antiproliferative activity of plasmid DNA/DXR complex on tumor cells co-cultured with RAW264.7 cells

RAW264.7 cells (2×10^5 cells/ml, 0.5 ml/well) and colon26/Luc cells (2×10^4 cells/ml, 0.5 ml/well) were placed in the upper and lower chambers of Transwell plates, respectively. Plasmid DNA, DXR or their complex was added to the upper side at a final concentration of 10 μg DNA/ml and 1 μg DXR/ml, and cells were incubated at 37 ℃ for 48 h. Then, colon26/Luc cells in the lower chambers were lysed in a cell lysis buffer (0.1 M Tris, 0.05% Triton X-100, 2 mM EDTA, pH 7.8). After centrifugation of the cell lysates, a part of the supernatant was mixed with a luciferase assay buffer (Piccagene, Toyo Ink, Tokyo, Japan), and the chemiluminescence produced was measured in a luminometer (Lumat LB9507, EG and G Berthold, Bad Wildbad, Germany). The luciferase activity was converted to the number of colon26/Luc cells as reported previously [34].

Hepatic metastatic model in mice

Colon26/Luc cells were trypsinized and suspended in HBSS. An abdominal incision was made and colon26/Luc cells (1×10^5 cells in 200 μl HBSS) were injected via the portal vein under anesthesia with diethyl ether. Then, the incision was sutured, and the mice were maintained under normal conditions after recovery from the anesthesia.

Immunohistochemistry and immunofluorescence

Tumor tissues of colon26/Luc cells were excised from the liver of the hepatic metastatic mice and were snap-frozen in isopentane. Acetone-fixed 10 μm-thick sections of tumor tissues were prepared using a cryostat. Then, nonspecific binding sites were blocked for 1 h at room temperature with 50% FBS in PBS. The sections were stained with anti-CD31 antibody (Biolegend, CA, USA) in PBS for 2 h, followed by incubation for 1 h with TRITC-conjugated goat anti-rat antibody (Santa Cruz Biotechnology, Inc., Santa Cruz, CA, USA). Then, the tumor sections were incubated with FITC-conjugated rat anti-mouse F4/80 antibody (AbD Serotec, Oxford, UK). Sections were analyzed by confocal microscopy.

IL-12 production in mice

At 14 days after inoculation of colon26/Luc cells, plasmid DNA in 5% dextrose was injected into the tail vein of tumor-bearing mice at a dose of 250 μg DNA/mouse in a free or complex form with DXR (25 μg/mouse). The dose of plasmid DNA was fixed to 250 μg/mouse throughout the experiments, because this dose was effective in inducing TNF-α after intravenous injection to mice [36]. At 6 h after injection, blood was collected from the vena cava of mice under anesthesia, and allowed to stand for 3 h at 4 °C. Then the samples were centrifuged at 3000 g for 20 min at 4 °C and the serum obtained was used for the measurement of IL-12. In addition, the isolated liver was washed with ice-cold saline, and homogenized in 2 ml PBS containing a cocktail of protease inhibitors (Sigma, St Louis, MO, USA). Serum and supernatants of tissue homogenates obtained after centrifugation at 15,000 g for 10 min were stored at −80 ºC until assay. The IL-12 concentration in these samples was measured using a Mouse IL-12 ELISA kit (Quantikine; R&D Systems, Minneapolis, MN, USA).

Tissue distribution of DXR

Mice with hepatic metastases of colon26/Luc cells received an intravenous injection of DXR (125 μg/mouse, corresponding to 6.25 mg/kg) or plasmid DNA/DXR complex (250 μg DNA and 125 μg DXR/mouse). This high dose of DXR was selected for sensitive detection of DXR after administration to mice. At predetermined intervals after injection, liver, heart and plasma samples were collected from mice. Then, DXR was extracted from each sample according to the method of Bachur et al. [37]. In brief, tissue samples were homogenized in a 0.3 M HCl–50% ethanol solution for 2 min and the homogenates were centrifuged at 20,000 g for 20 min at 4 °C. The DXR concentration in the supernatant was determined fluorometrically. Tissue samples from untreated mice were used for the estimation of background fluorescence. The DXR concentration in tumor tissues was determined at 15 min after injection of DXR or plasmid DNA/DXR complex.

Accumulation of DXR in tumor tissue

DXR or plasmid DNA/DXR complex was injected into mice with hepatic metastases of colon26/Luc cells as described above, and the tumor tissues were excised and snap-frozen in isopentane at 15 min after injection. Acetone-fixed 10 μm-thick sections of tumor tissues were prepared using a cryostat. DXR in the sections was detected by measuring the fluorescence intensity of DXR at excitation and emission wavelengths of 543 and 568 nm, respectively.

Antitumor effect of plasmid DNA/DXR complex in a hepatic metastasis model

At 8 days after inoculation of colon26/Luc cells into the portal vein, plasmid DNA (250 μg/mouse), DXR (25 or 125 μg/mouse) or their complex (250 μg DNA and 25 or 125 μg DXR/mouse) was injected into the tail vein of mice. At 5 days after injection, the mice were killed and the liver was excised and homogenized in a lysis buffer. The homogenate was centrifuged and the luciferase activity of the supernatant was measured as described above as an indicator of the number of colon26/Luc cells in the organ.

Statistical analysis

Differences were statistically evaluated by one-way ANOVA and post hoc Tukey's tests. The level of statistical significance was set at $P < 0.05$.

I-3 Results

I-3-a. Preparation of plasmid DNA/DXR

Fig. 1 shows the agarose gel electrophoresis of CpG plasmid DNA added with different amounts of DXR. Plasmid DNA showed several bands, each of which represented supercoiled, open circular and linear forms. The mobility of the CpG plasmid DNA decreased as the amount of DXR added to the DNA increased. In addition, the greater the amount of DXR added the weaker the band intensity of plasmid DNA became, suggesting that the intercalation of ethidium bromide to DNA base pairs is inhibited by the intercalation of DXR. Fig. 2 shows the apparent size of the plasmid DNA/DXR complexes prepared at different mixing ratios. The apparent size of the complex gradually increased with an increasing amount of DXR, and it almost reached a plateau of about 500 nm at a mixing ratio of 1:0.5 (DNA:DXR, on a weight basis).

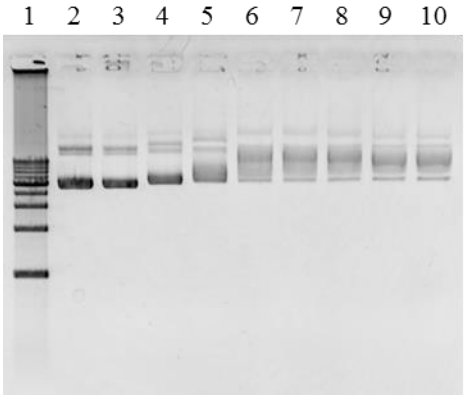

FIGURE 1. Agarose gel electrophoresis of plasmid DNA and plasmid DNA/DXR complex. Plasmid DNA (pcDNA3.1) or its complex (1 μg DNA/lane) was run on 1% agarose gel and visualized with ethidium bromide. Lane 1, DNA size standard (1 kb DNA ladder; Takara, Tokyo, Japan); lanes 2–3, plasmid DNA; lanes 4–10, plasmid DNA/DXR complex at different mixing ratios (DNA/DXR, on a weight basis: lane 4, 1:0.02; lane 5, 1:0.04; lane 6, 1:0.06; lane 7, 1:0.08; lane 8, 1:0.1; lane 9, 1:0.5; lane 10, 1:1).

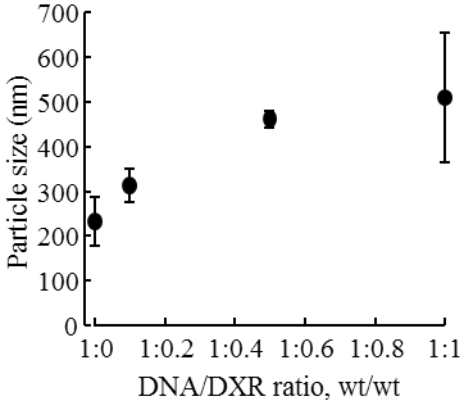

FIGURE 2. Apparent particle size of plasmid DNA/DXR complex at different mixing ratios. To a 5% dextrose solution of plasmid DNA were added different amounts of DXR, and the apparent size of the resulting complexes was measured using a Zetasizer. Results are expressed as mean ± SD of three independent measurements.

I-3-b. Effect of plasmid DNA/DXR on TNF-α secretion from, and proliferation of, RAW264.7 cells

To investigate whether plasmid DNA/DXR complex is as effective in activating RAW264.7 cells as plasmid DNA alone, TNF-α secretion was measured at 8 h after addition of plasmid DNA/DXR complexes to RAW264.7 cells. A high concentration (about 2700 pg/ml) of TNF-α was detected in the supernatant of RAW264.7 cells treated with CpG plasmid DNA (Fig. 3a). Similar levels of TNF-α were released from cells treated with CpG plasmid DNA/DXR prepared at 1:0.01 or 1:0.1. Increasing the amount of DXR to 1:0.5 or 1:1 greatly reduced the TNF-α secretion. Fig. 3b shows the viability of RAW264.7 cells

determined by an MTT assay. The addition of CpG plasmid DNA or CpG plasmid DNA/DXR complex prepared at ratios from 1:0.01 to 1:0.5 produced hardly any reduction in the number of cells. Increasing the incubation time up to 48 h slightly increased the cytotoxic effects of the complex to the cells (data not shown). On the other hand, the complex prepared at the highest ratio produced a marked reduction in the number of cells, suggesting that this complex containing a large amount of DXR is highly toxic to RAW264.7 cells. This cytotoxic effect would be responsible for the reduced TNF-α production in RAW264.7 cells when added along with CpG plasmid DNA/DXR complex prepared at higher ratios of DXR. Based on these observations, plasmid DNA/DXR complexes were prepared at mixing ratios of 1:0.1 and 1:0.5 (DNA:DXR, wt/wt) in the subsequent experiments.

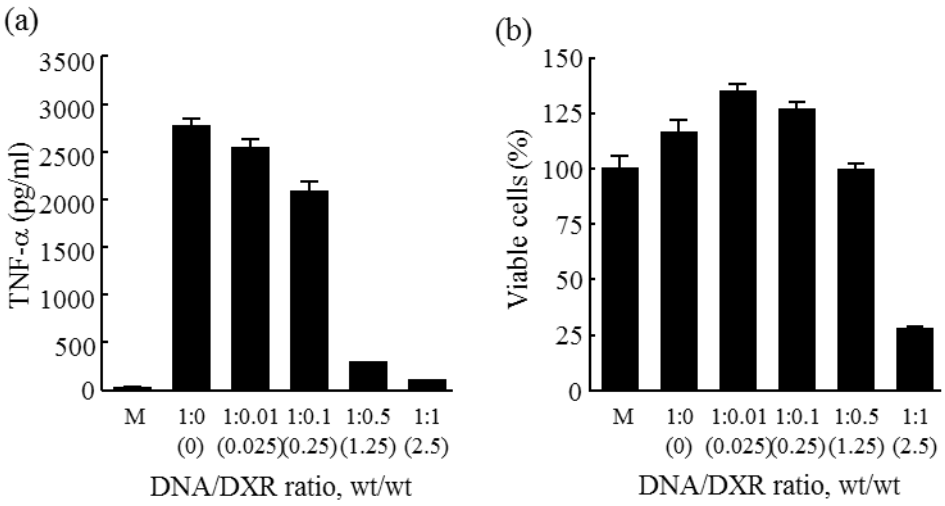

FIGURE 3. TNF-α secretion (a) and number of viable cells (b) after addition of plasmid DNA/DXR complex to RAW264.7 cells. (a) Concentration of TNF-α in culture media was measured at 8 h after addition of plasmid DNA (pcDNA3.1) or its complex with DXR to cells at a final concentration of 2.5 μg DNA/ml. (b) Number of viable cells were measured by MTT assay at 8 h and were converted to a percentage of the medium-treated (M, control) cells. Results are expressed as mean ± SD of three independent measurements.

I-3-c. Anti-proliferative activity of plasmid DNA/DXR complex on colon26/Luc cells

Fig. 4 shows the number of colon26/Luc cells co-cultured with RAW264.7 cells using Transwell plates. The addition of CpG plasmid DNA significantly ($P < 0.05$) inhibited the proliferation of colon26/Luc cells. On the other hand, non-CpG plasmid DNA had no significant effect on the number of tumor cells. Free DXR also reduced the number of tumor cells. CpG plasmid DNA/DXR (1:0.1) complex produced a greater reduction in the number of tumor cells compared with free DXR, CpG plasmid DNA or non-CpG plasmid DNA/DXR complex. These results suggest that DXR and CpG plasmid DNA exhibit at least additive effects in inhibiting the proliferation of tumor cells co-cultured with RAW264.7 cells.

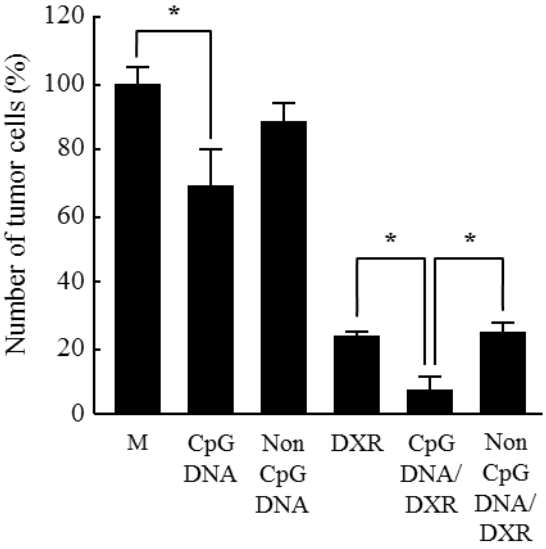

FIGURE 4. Inhibition of proliferation of colon26/Luc cells by plasmid DNA/DXR complex. RAW264.7 and colon26/Luc were placed in the upper and lower chambers of Transwell plates, respectively. Plasmid DNA (CpG DNA, pcDNA3.1; non-CpG DNA, pCPG-mcs), DXR, or their complex was added to the upper side at a final concentration of 10 μg DNA/ml and 1 μg DXR/ml (1:0.1, on a weight basis). The luciferase activity of colon26/Luc cells was measured at 48 h as an indicator of the number of tumor cells, and was converted to a percentage of the medium-treated (M, control) cells. Results are expressed as mean ± SD of three independent measurements. $^{*}P < 0.05$.

I-3-d. Immunostaining of tumor-associated macrophages and vascular endothelial cells in tumor tissue

It has been reported that tumor tissues contain many infiltrating immune cells, such as tumor-associated macrophages (TAMs). To confirm whether colon26/Luc tumor contains significant numbers of tumor-infiltrating immune cells, TAMs as well as vascular endothelial cells were immunostained in tumor sections (Fig. 5). Many endothelial cells were detected in the sections, and these were surrounded with lots of F4/80-positive cells.

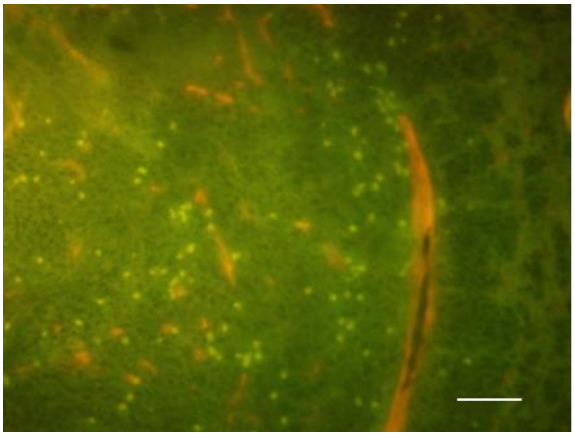

FIGURE 5. Immunostaining of tumor-associated macrophages and vascular endothelial cells on a section of colon26/Luc tumor. Tumor tissues of colon26/Luc cells were excised from the liver of mice with hepatic metastases, and thin sections were prepared using a cryostat. The sections were stained with anti-CD31 antibody (endothelial cells, red) and anti-mouse F4/80 antibody (macrophages, green). Bar, 100 μm.

I-3-e. IL-12 production after intravenous injection of plasmid DNA/DXR complex in mice with hepatic metastases of colon26/Luc cells

Fig. 6a shows the serum concentration of IL-12 in mice with hepatic metastases of colon26/Luc cells after intravenous injection of plasmid DNA. CpG plasmid DNA induced a high level of IL-12 in both serum and liver in a manner that depended on the dose of plasmid DNA. In marked contrast, non-CpG plasmid DNA induced no significant increase in the IL-12 concentration even at the high dose of 250 μg/mouse. Similar experiments were then carried out using plasmid DNA/DXR. Fig. 6b shows the concentration of IL-12 in serum and liver after intravenous injection of CpG plasmid DNA, DXR or CpG

plasmid DNA/DXR. No significant IL-12 was detected in serum or liver of mice receiving 5% dextrose solution or free DXR. On the other hand, CpG plasmid DNA/DXR complex produced significant amounts of IL-12 both in serum and liver, even though the levels of the complex were lower than those of CpG plasmid DNA containing no DXR. Increasing the amount of DXR reduced the amounts of IL-12, which was in agreement with the results of TNF-α release from RAW264.7 cells (Fig. 3a).

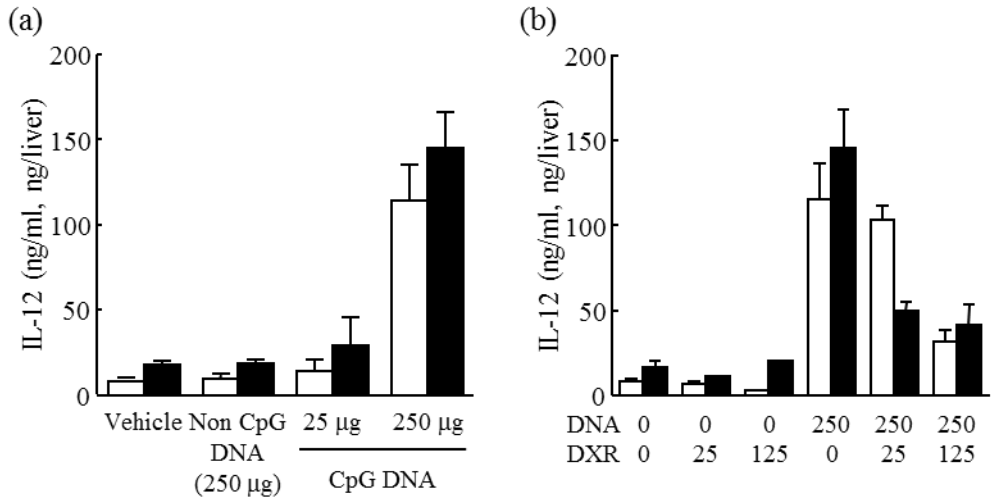

FIGURE 6. IL-12 concentration in the serum and liver of mice with hepatic metastases after intravenouos injection of plasmid DNA (a) or plasmid DNA/DXR complex (b). (a) Mice with hepatic metastases of colon26/Luc cells were injected with CpG- or non-CpG plasmid DNA (pcDNA3.1 and pCpG-mcs, respectively) at a dose of 25 or 250 μg/mouse. (b) Mice with hepatic metastases of colon26/Luc cells were injected with CpG plasmid DNA (pcDNA3.1), DXR or their complex at the indicated doses (μg/mouse). At 6 h after injection, serum and liver samples were collected and the concentration of IL-12 was measured by ELISA. Results are expressed as mean ± SD of three mice. Open bars, serum; closed bars, liver.

I-3-f. Tissue distribution of DXR in mice with hepatic metastases of colon26/Luc cells

Fig. 7a–c shows the concentration of DXR in serum, liver and heart of mice after intravenous injection of DXR or CpG plasmid DNA/DXR (1:0.5) complex. Free DXR disappeared very quickly from the blood circulation, and distributed to the heart and liver. The administration in the form of CpG plasmid DNA/DXR produced a slightly higher concentration of DXR in the blood. In addition, the amount of DXR delivered to the liver containing metastatic tumor cells was significantly ($P < 0.05$) greater for CpG plasmid DNA/DXR than for free DXR. To confirm whether DXR is delivered to tumor tissues in the liver, the concentration of DXR in tumor tissues was measured (Fig. 7d). This quantitative analysis showed that DXR administered in the form of CpG plasmid DNA/DXR complex was delivered to the tumor tissue more efficiently than that administered in the free form. Fig. 7e and f shows the DXR-derived fluorescence in a section of tumor tissues after intravenous injection of DXR or CpG plasmid DNA/DXR, respectively. In agreement with the quantitative results (Fig. 7d), a greater amount of DXR was detected in the tumor tissues when DXR was injected as CpG plasmid DNA/DXR, suggesting that plasmid DNA is an effective carrier for delivering DXR efficiently to tumor tissues.

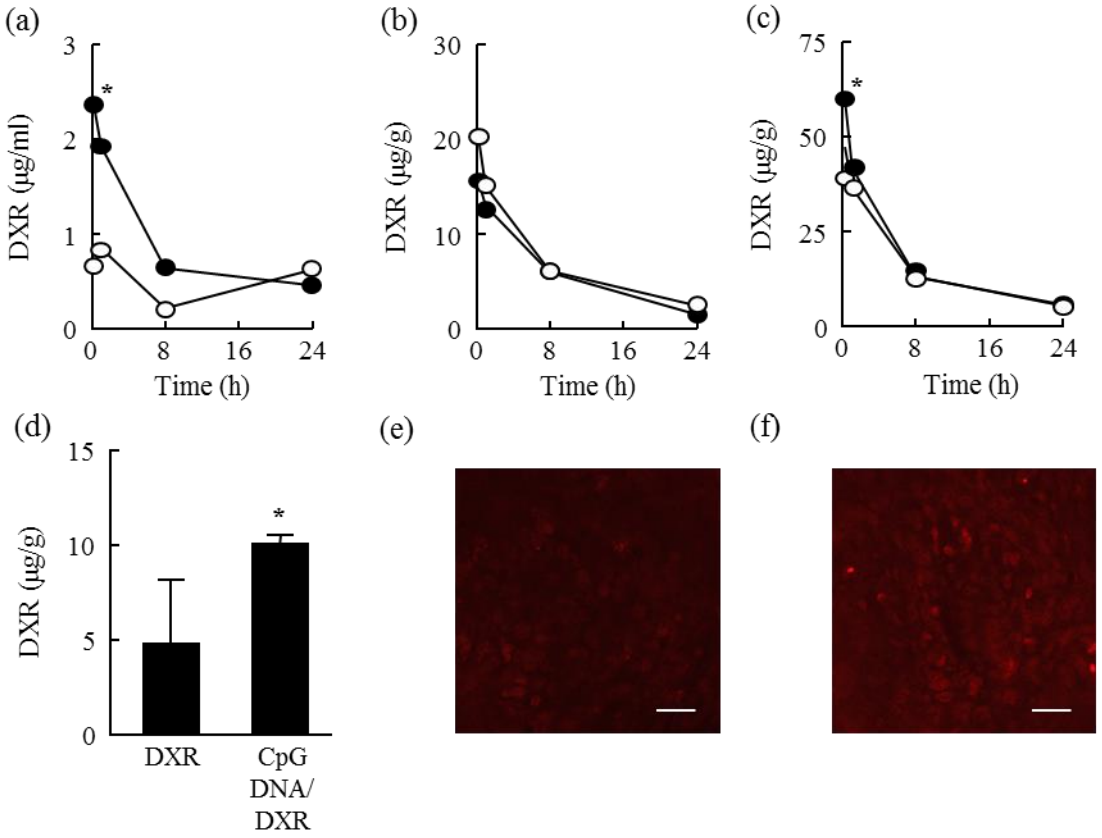

FIGURE 7. Tissue distribution of DXR after intravenous injection of DXR or CpG plasmid DNA/DXR complex into mice with hepatic metastases. Mice with hepatic metastases of colon26/Luc cells were injected with DXR (○) or CpG plasmid DNA (pcDNA3.1)/DXR complex (●) at a dose of 125 μg DXR and 250 μg DNA/mouse. (a–c) Serum (a), heart (b) and liver (c) samples were collected, and the DXR concentrations were determined fluorometrically. Results are expressed as mean + SD of three mice. $*P < 0.05$ compared with the DXR-injected group. (d) At 15 min after injection, tumor tissues in the liver were collected and the DXR concentration in the tumor was determined. Results are expressed as mean ± SD of four mice. $*P < 0.05$ compared with the DXR-injected group. (e,f) At 15 min after injection, tumor tissues were excised and frozen sections were prepared using a cryostat. (e) DXR, (f) CpG plasmid DNA/DXR complex. Bars, 10 μm.

I-3-g. Inhibition of hepatic metastases of colon26/Luc cells by CpG plasmid DNA/DXR complex

Fig. 8 shows the number of colon26/Luc cells in the liver of mice. Under the conditions used, about $2.17 \pm 0.55 \times 10^6$ cells were found in the liver at 13 days after inoculation of tumor cells. A single dose of CpG plasmid DNA significantly reduced the number to $6.80 \pm 5.78 \times 10^5$ cells. The inhibitory effect of CpG plasmid DNA/DXR (1:0.1) complex was significantly greater than that of DXR or CpG plasmid DNA, indicating that the complex exhibits at least an additive effect in inhibiting the proliferation of tumor cells in mouse liver. On the other hand, the separate administration of DXR (25 or 125 μg/mouse) and CpG plasmid DNA (250 μg/mouse) with 1 h-interval was less effective than their administration as a complex (data not shown). The reduction obtained with the complex was as great as that of 125 μg free DXR. The complex prepared at the ratio of 1:0.5 inhibited the proliferation of tumor cells to a level of less than 1% ($3.86 \pm 4.81 \times 10^3$ cells) of that in untreated mice. Non-CpG plasmid DNA had a much weaker effect on the number of tumor cells than the CpG plasmid DNA (data not shown), suggesting that the CpG

motifs in plasmid DNA have some positive effects in inhibiting the proliferation of tumor cells. Because CpG plasmid DNA/DXR complex exhibited better effects than CpG plasmid or DXR, these results strongly suggest that the combination of DXR and CpG motif-containing plasmid DNA exhibits additive, if not synergistic, effect on hepatic metastases of tumor cells.

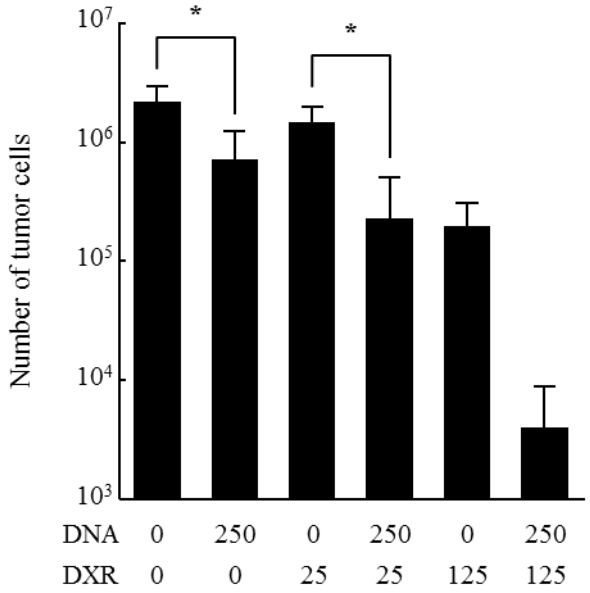

FIGURE 8. Number of colon26/Luc cells in the liver of mice receiving plasmid DNA, DXR or their complex. Colon26/Luc cells were inoculated into mice via the portal vein. At 8 days after inoculation, CpG plasmid DNA, DXR or its complex at the indicated doses (μg/mouse) was injected into the tail vein of the mice. Five days later, the mice were killed and the luciferase activity in the liver was measured. Results are expressed as mean ± SD of four mice. $^*P < 0.05$.

I-4 Discussion

The use of macromolecules in the treatment of cancer has become a popular method to deliver low-molecular-weight anticancer agents to solid tumors because the conjugation to, or complexation with, macromolecules greatly alters the tissue distribution of the agents [19]. The pioneer work by Trouet et al. used CT DNA as a carrier for DXR, and reported that the use of CT DNA is a promising approach for delivering DXR to tumor cells [13, 25, 26]. However, the tissue distribution of DXR was not properly examined in these studies. The present study has demonstrated that the delivery of DXR to tumor tissues in mouse liver was significantly increased by complex formation with CpG plasmid DNA (Fig. 7). CpG plasmid DNA/DXR exhibited an increased concentration in plasma but a reduced concentration in heart, suggesting that the distribution of DXR can be at least partly controlled by the use of plasmid DNA. However, the control of the distribution seemed not to be so effective, because plasmid DNA hardly distributed to the heart whereas significant amounts of DXR were detected in that organ after injection of CpG plasmid DNA/DXR. Thus, an additional approach to controlling the release of DXR would be effective in increasing not only the delivery of DXR to tumor tissues but also the therapeutic efficacy of the DNA/DXR complex.

After intravenous injection, plasmid DNA accumulates extensively in the liver [38] because liver nonparenchymal cells, including Kupffer cells and sinusoidal endothelial cells, take up plasmid DNA and other polyanions through scavenger receptor-like mechanisms [38, 39]. RAW264.7, a mouse macrophage-like cell line, and tissue macrophages, such as splenic macrophages, are known to take up DNA. In previous studies, the uptake of plasmid DNA by these types of cells was repeatedly reported [29-33]. The distribution of DXR after intravenous injection in the form of CpG plasmid DNA/DXR complex showed a high accumulation in tumor tissues in the liver (Fig. 7d–f). This increased distribution of DXR to tumor tissues may be due to facilitated accumulation of plasmid DNA/DXR complex in tumor

tissues, because the EPR effect of solid tumors allows macromolecules and small particles, such as PEGylated liposomes, to selectively accumulate in the tissues [24]. The increase in the apparent size of plasmid DNA by the addition of DXR (Fig. 2) would be explained by experimental evidence that intercalating agents unwind the double helices of DNA and extend it [40]. The length of CpG and non-CpG plasmid DNA used in the present study was different each other, but the hydrodynamic size measured using dynamic laser scattering was comparable (data not shown). Furthermore, plasmid DNA would undergo enzymatic degradation after administration, which would lead to the reduction in size and facilitate the accumulation of plasmid DNA/DXR complex to tumor tissues. However, the increased distribution of DXR to tumor tissues could also be due to selective uptake of the complex by cells present in tumor tissues. TAMs are a candidate for the cells that are responsible for the uptake of plasmid DNA by tumor tissues. In the present study, we found that a number of F4/80-positive cells had infiltrated tumor tissues (Fig. 5). Although the involvement of TAMs and other infiltrating immune cells in the uptake of plasmid DNA complex by tumor tissues has not been confirmed, their ability to take up polyanions would suggest that they, at least partly, contribute to the efficient uptake of DXR administered as a plasmid DNA/DXR complex by tumor tissues.

We detected the release of TNF-α from RAW264.7 cells after addition of CpG plasmid DNA or its complex with DXR (Fig. 3), and the release of IL-12 in tumor-bearing mice after intravenous injection of CpG plasmid DNA or its complex with DXR (Fig. 6). The low production of IL-12 by non-CpG plasmid DNA clearly demonstrated that the production was mediated by the CpG motifs in plasmid DNA. Previous studies conducted in my laboratory or by others using mice without tumor have also shown that a variety of cytokines, including TNF-α, IL-12 and IL-6, is produced in mice after administration of CpG motif-containing DNA. The cytokines produced are effective in inhibiting the proliferation of tumor cells in a variety of experimental settings. The survival of tumor-bearing mice was significantly increased by administration of CpG DNA complexed with cationic liposomes [34]. These pieces of experimental evidence indicate that CpG plasmid DNA is much better than CT DNA or sperm DNA, because it can stimulate the innate immune system to release proinflammatory, antitumor cytokines. These responses may raise a concern about severe side effects, such as cytokine storm, in which extremely high levels of cytokines are produced. However, the levels of cytokines were not so high as those obtained by LPS, and no obvious symptoms of cytokine storm, such as high fever and extreme fatigue, were seen in mice receiving plasmid DNA or plasmid DNA/DXR complex.

One concern involving the use of CpG plasmid DNA/DXR complex is that the target cells for delivery of such complex, i.e., TAMs and other cells having the ability to take up polyanions including tumor-infiltrating dendritic cells, are killed by DXR and, therefore, cannot release cytokines. This concern would also be applicable to liposomal formulations of DXR, such as Doxil®, because such formulations are believed to be taken up by TAMs, then release active DXR [41, 42]. If this is the case, TAMs are considered to be resistant to the cytotoxic activity of DXR. We observed that 1.25 μg DXR/ml produced only a slight reduction in the number of RAW264.7 cells when DXR was added as CpG plasmid DNA/DXR complex, but 1 μg DXR/ml killed more than 70% of colon26/Luc cells (Fig. 4). The release of TNF-α from RAW264.7 cells added with CpG plasmid DNA/DXR as well as its additive effects on the proliferation of colon26/Luc cells strongly suggests that RAW264.7 cells are resistant to the cytotoxic activity of DXR when added as a complex form with plasmid DNA. Increasing the mixing ratio of DXR in the complex, however, significantly reduced the number of RAW264.7 cells, indicating that the amount of DXR taken up by TAMs should not be too high in order to obtain additive effects of CpG DNA-mediated release of cytokines and cytotoxic effects of DXR. In a mouse model of hepatic metastasis, we confirmed

that the complex is very effective in inhibiting tumor growth, indicating that the simultaneous delivery of the immunostimulatory signal and the anticancer agent DXR can be achieved by CpG plasmid DNA/DXR complex. In early studies using CT DNA or sperm DNA as a carrier of anticancer agents, the cytotoxic effects of such complexes were discussed in relation to the high endocytic and mitotic activities of tumor cells [25, 43]. Another concern about the delivery of such complexes to macrophages is the decomposition or inactivation of DXR in cells. However, a previous study clearly demonstrated that DXR was chemically stable for up to 26 h when incubated with lysosomal fractions of rat liver [41]. On the other hand, the consequences of the uptake of plasmid DNA/DXR complex by liver nonparenchymal cells need additional studies.

Plasmid DNA has a number of advantages over other polymers as a drug carrier. It shares most of the characteristics of mammalian genomic DNA, and all the components of plasmid DNA are found in the genomic DNA. Therefore, plasmid DNA is degraded by DNases to oligodeoxynucleotides and will not accumulate in the body even when administered frequently. The administration of plasmid DNA to humans has already been carried out in clinical trials of in vivo gene therapy, and no serious side effects have been reported thus far. In addition, the size and sequence, including the CpG motif, are easily controlled, and a large amount of plasmid DNA can be produced in bacteria with no marked size distribution.

Possible drawbacks of plasmid DNA as a carrier for anticancer agents include the contamination of LPS, instability, and the limitation of anticancer agents that can be delivered by DNA. These problems could be solved by the use of synthetic DNA instead of bacterially derived plasmid DNA. Chemically modified DNA analogues resistant to nucleases are available, and the construction of highly ordered nanostructures has recently been reported [44], which could result in favorable tissue distribution characteristics like plasmid DNA. These DNA-based structures can be designed to have functional groups or unique properties that could be used to conjugate or load a variety of anticancer agents.

I-5 Conclusion

I have shown that CpG plasmid DNA/DXR complex is effective in inhibiting the proliferation of tumor cells under conditions where cells responding to CpG motifs and releasing proinflammatory cytokines are present. Its strong therapeutic activity was revealed to be due, in part, to the production of cytokines, such as IL-12 and TNF-α, and the efficient delivery of DXR to tumor tissues. These results shed new light on plasmid DNA as a suitable carrier of anticancer agents with high biocompatibility, biodegradability and plasticity.

Chapter II

Development of antigen delivery system based on immunostimulatory-motif containing DNA hydrogel consisting of polypod-like structured DNA

II Introduction

In Chapter I, I demonstrated that CpG motif-containing DNA is effective as a carrier for anticancer agent using plasmid DNA. Considering the risk of the contamination of LPS in clinical application, in Chapter II, I used synthetic oligodeoxynucleotides (ODNs) which also have various advantages as DDS carriers including ease of chemical synthesis on a large scale, high stability and biodegradability [12]. Structural DNA nanotechnology using ODNs has progressed dramatically since Seeman's pioneer work in 1980s [45]. ODNs are blocks for nanoconstruction because of its predictable conformation and programmable intra-and intermolecular Watson-Crick base-parting interactions. Various types of DNA nanostructures with increasing complexity have been developed by designing the sequences of ODNs [46-49]. This structural DNA nanotechnology seems to be useful for the development of ODN-based functional DDS carriers which are safe and applicable for various drugs including ones with little interaction with DNA. Hence I have worked on the development of DNA hydrogel which is enzymatically catalyzed assembly of CpG motif-containing X-shaped DNA based on ODNs, and demonstrated its effectiveness as a DDS carrier for DXR on inhibition of the growth of subcutaneous tumors [50]. My laboratory extended these results and recently developed a novel method to prepare an enzyme-free, self-gelling and injectable DNA hydrogel consisting of polypod-like structured DNA prepared using CpG motif-containing ODNs. Intradermal injection of this immunostimulatory DNA hydrogel (sDNA hydrogel) loaded with ovalbumin as a model antigen showed high potency and low toxicity as a vaccine adjuvant for cancer immunotherapy [15]. However, the potential of sDNA hydrogel as a carrier for mucosal delivery or allergy immunotherapy has not been investigated so far.

Therefore, in Chapter II, I have developed a sDNA hydrogel-based advanced antigen delivery system. In Section 1, the effectiveness of sDNA hydrogel as a nasal antigen delivery carrier for allergy immunotherapy was investigated. In Section 2, I aimed to optimize the sDNA hydrogel based antigen delivery system by improving the release profile of antigen from the hydrogel.

Chapter II

Section 1

Development of nasal antigen delivery system based on immunostimulatory DNA hydrogel for allergy immunotherapy

II-1-1 Introduction

Ligation of TLR9 with CpG motif results in the release of tumor necrosis factor (TNF)-α , interleukin (IL)-12, and other proinflammatory cytokines, and in the stimulation of humoral and cellular immune responses [5-8]. CpG DNA-induced secretion of Th1 cytokines such as IL-12 and IFN-γ converts uncommitted T-cells (Th0) to T helper 1 cells (Th1), which suppress the function of Th2 cells [11]. At least two mechanisms for CpG DNA as an allergy vaccine adjuvant are known. The first is reduced Th2 responses manifested as reduced activation of basophils and eosinophils, and reduced class-switching of B-cells to produce IgE [5, 11]. The second is CpG DNA-induced humoral immunity such as competition of allergen-specific IgG and IgA with IgE for allergen binding [51, 52]. Previous clinical studies have shown that subcutaneous injection of CpG DNA conjugated with ragweed pollen antigen was effective for preventing ragweed seasonal allergic rhinitis in humans [53, 54].

Allergic rhinitis is a global health problem affecting 10–20% of the population [55]. The incidence of allergic rhinitis caused by Japanese cedar pollen (JCP) is estimated to be 30–40% among adult Japanese population [56]. Although symptomatic therapy with pharmacological agents has been a common treatment for allergic rhinitis thus far, considerable attention has been paid to allergen-specific immunotherapies that induce long-term remission [57]. At present, allergy immunotherapy involves 3–5 years of subcutaneous injections, but a short-term and self-administrable mucosal immunotherapy such as intranasal or sublingual vaccines will be ideal for patients [58]. Immunotherapy with an immunostimulatory adjuvant such as CpG DNA is expected to induce effective immune responses for shorter mucosal immunotherapy.

As I described above, my laboratory has developed a ligase-free, self-gelling and injectable CpG motif-containing immunostimulatory DNA hydrogel (sDNA hydrogel). This self-gelling DNA hydrogel can be administered to cavities as a spray, therefore it could be a useful delivery system for intranasal vaccines. However its application for mucosal delivery has not been investigated.

In this section, I developed nasal antigen delivery system based on sDNA hydrogel consisting of polypod-like structured DNA for allergic rhinitis. To the best of my knowledge, this is the first attempt of a newly designed self-gelling immunostimulatory CpG DNA hydrogel loaded with Cryj1, a major JCP allergen (Cryj1/sDNA hydrogel). The physicochemical properties and biological activity of the Cryj1/sDNA hydrogel were examined after intranasal administration to mice, to evaluate the potential of the sDNA hydrogel as an intranasal delivery system to induce immunotherapeutic effects against allergic rhinitis.

II-1-2 Materials and Methods

Chemicals

RPMI 1640 medium was obtained from Nissui Pharmaceutical (Tokyo, Japan). Fetal bovine serum (FBS) was obtained from MP Biomedicals (Eschwege, Germany). Cryj1 was extracted from JCP by stirring in 0.125 M $NaHCO_3$ solution (pH8.0) for 1 h at room temperature, and the extract was purified by centrifugation at 15,000 g for 30 min and ultrafiltration of the supernatant using a 10-kDa filter. The content of purified Cryj1 was determined by an ELISA kit for Cryj1 purchased from Nichinichi Pharmaceutical (Mie, Japan). Cryj1 was labeled with fluorescein isothiocyanate (FITC; fluorescein isothiocyanate isomer 1, Sigma-Aldrich, St. Louis, MO, USA) to obtain FITC-Cryj1. All other chemicals were of the highest grade available and used without further purification.

Cell culture

The murine macrophage-like cell line RAW264.7 was obtained from the American Type Culture Collection (Rockville, MD, USA). Cells were grown in RPMI 1640 medium supplemented with 10% heat-inactivated FBS, 0.15% $NaHCO_3$, 100 units/ml penicillin, 100 μg/ml streptomycin, and 2 mM L-glutamine at 37°C in humidified air containing 5% CO2.

Animals

Male BALB/c mice (5 weeks old) were purchased from Japan SLC, Inc. (Shizuoka, Japan). Animals were maintained under conventional housing conditions. All animal experiments were approved by the Animal Experimentation Committee of the Graduate School of Pharmaceutical Sciences, Kyoto University.

Preparation of polypodna and DNA hydrogel loaded with Cryj1

All phosphodiester oligodeoxynucleotides (ODNs) were purchased from Integrated DNA Technologies, Inc. (Coralville, IA, USA). The hexapodna and DNA hydrogel was designed and prepared using the ODNs as reported in previous study of my laboratory [15]. In brief, three immunostimulatory hexapodna (sHexa) with potent CpG motifs, and three non-immunostimulatory hexapodna (nsHexa) with no CpG motifs were prepared. sHexa-1 and sHexa-2 were designed to have complementary 5′-ends. nsHexa-1 and nsHexa-2 were also designed similarly. The sequence of sHexa-3 was identical to that of sHexa-2 except for their 5′-ends, and sHexa-3 did not have a 5′-end complementary to sHexa-1.

The formation of hexapodna was confirmed by 6% polyacrylamide gel electrophoresis (PAGE). Immunostimulatory and non-immunostimulatory DNA hydrogels (sDNA hydrogel and nsDNA hydrogel, respectively) were obtained by mixing equimolar amounts of sHexa-1 and sHexa-2 or nsHexa-1 and nsHexa-2, respectively, at an initial concentration of 0.1 or 0.3 mM DNA (7 μg/μl DNA or 22 μg/μl DNA, respectively). A hexapodna solution was also prepared as a control by mixing sHexa-1 and sHexa-3. To prepare the Cryj1-loaded DNA hydrogels (Cryj1/sDNA hydrogel and Cryj1/nsDNA hydrogel), Cryj1 was added to sHexa-1 and sHexa-2 or nsHexa-1 and nsHexa-2, respectively, before mixing. Hydrogel formation was briefly confirmed by adding a solution containing blue dextran (Sigma-Aldrich), which does not instantly diffuse into hydrogels, or by 6% PAGE as previously reported [15].

Observation of the inner structure of the sDNA hydrogel and Cryj1/sDNA hydrogel by scanning electron microscopy

The inner structures of the 0.1 mM and 0.3 mM Cryj1/sDNA hydrogels were observed using a field-emission scanning electron microscope (FE-SEM: S4700; HITACHI, Japan) as previously described [15]. In brief, the samples were fixed with 2% glutaraldehyde at room temperature overnight, dehydrated with increasing concentrations of ethanol that was then replaced with butyl alcohol, and then freeze-dried. The dried material was cracked with a knife, and the inner structure of the DNA hydrogels was observed.

Cryj1 release from DNA hydrogel in vitro

FITC-Cryj1 was mixed with sHexa-1 and sHexa-2 solutions, and 0.1 mM and 0.3 mM sDNA hydrogels containing FITC-Cryj1 were prepared as described above. As a control, FITC-Cryj1 was mixed with sHexa-1 and sHexa-3 solutions, and 0.1 mM or 0.3 mM sHexa solution containing FITC-Cryj1 (FITC-Cryj1+sHexa) was prepared. Then, the FITC-Cryj1/sDNA hydrogel or FITC-Cryj1+sHexa was placed into the upper chamber of a Transwell (Product#3460, 0.4-μm pore size; Corning Inc., Corning, NY, USA), and 1000 μl of PBS was added into the bottom chamber, followed by incubation at 37°C. At predetermined time points, fluorescence images of FITC-Cryj1/sDNA hydrogel were obtained using LAS3000 system (Fujifilm, Tokyo, Japan), and the fluorescence intensity of the receiver solution was measured in a Wallac1420 ARVO MX-2 Multilabel Counter (Perkin-Elmer, Boston, MA, USA).

IL-12 release from RAW264.7 cells

RAW264.7 cells were plated on 24-well culture plates at a density of 5×10^5 cells/ml (2.5×10^5 cells/well) and cultured for 24 h before use. ssODN (a mixture of CpG Hex.-1-1 and CpG Hex.-3-1), sHexa (a mixture of sHexa-1 and sHexa-3), sDNA hydrogel, nsDNA hydrogel, ssODN with Cryj1 (Cryj1+ssODN), sHexa with Cryj1 (Cryj1+sHexa), sDNA hydrogel or nsDNA hydrogel physically mixed with Cryj1 (Cryj1+sDNA hydrogel or Cryj1+nsDNA hydrogel, respectively), or Cryj1/sDNA hydrogel was diluted in Opti-MEM buffer (Life Technologies, Carlsbad, CA, USA) to a concentration of 100 μg/ml DNA and 20 μg/ml Cryj1, before it was added to the cells. The cells were incubated for 16 h, and the supernatants were collected and stored at -80°C until assayed. The level of IL-12p40 in the supernatant was determined by enzyme-linked immunosorbent assay (ELISA) by using an OptEIATM set (BD Biosciences, San Diego, CA, USA).

Cellular uptake of FITC-Cryj1 by RAW264.7 cells

RAW264.7 cells were plated on 96-well culture plates at a density of 5×10^5 cells/ml (5×10^4 cells/well) and cultured for 24 h before use. The cells were then washed twice with 100 μl of PBS and incubated with FITC-Cryj1, FITC-Cryj1 with ssODN (FITC-Cryj1+ssODN), FITC-Cryj1 with sHexa (FITC-Cryj1+sHexa), FITC-Cryj1 with sDNA hydrogel (FITC-Cryj1+sDNA hydrogel), or FITC-Cryj1/sDNA hydrogel at 37°C or 4°C. At 3 h after addition, the cells were washed three times with 200 μl PBS. Then, fluorescent intensity of the cells was determined by flow cytometry (FACSCalibur; BD Biosciences, San Jose, CA, USA) using CellQuest software (version 3.1; BD Biosciences), and the mean fluorescence intensity (MFI) was calculated as an indicator of the cellular uptake of FITC-Cryj1.

Distribution and clearance of Cryj1/DNA hydrogel after intranasal administration to mice

A mixed solution of sHexa and FITC-Cryj1 (FITC-Cryj1+sHexa) (50 μg DNA, 10 μg Cryj1/mouse) or FITC-Cryj1/sDNA hydrogel (50 μg DNA, 10 μg Cryj1/mouse) was intranasally (i.n.) administered to BALB/c mice by using a micropipette, under anesthesia with pentobarbital at a concentration of 0.1 mM DNA. At 0.5, 3, and 6 h after administration, the mice were killed, and nasal

lavage fluid (NLF) was collected by washing the nasal cavity with 800 μl of PBS. The concentration of DNA in the NLF was measured at 260 nm by NanoDrop™ 2000 (Thermo Scientific, Waltham, MA, USA), and the concentration of Cryj1 was evaluated by measuring the fluorescence intensity of the samples in a Wallac1420 ARVO MX-2 Multilabel Counter. In different sets of mice, the distribution of DNA was observed using LAS3000 after staining of DNA remaining in the nasal cavity with SYBR Gold (Life Technologies, Carlsbad, CA, USA).

IL-12 production in serum and NLF after intranasal administration of the sDNA hydrogel to mice

Saline, ssODN, or sDNA hydrogel was administered i.n. to BALB/c mice by using a micropipette at a dose of 50 μg DNA/mouse (DNA concentration: 0.1 mM, 6.8 μl/mouse) under anesthesia with pentobarbital. At 6 h after administration, the mice were killed, and their blood was collected to obtain serum after centrifugation. NLF was also collected by washing the nasal cavity with 1000 μl of PBS. The level of IL-12p40 in the serum and NLF was determined by ELISA.

IL-12 and IFN-γ release from spleen cells after immunization of mice

Cryj1, Cryj1 and ssODN (Cryj1+ssODN), Cryj1 and sHexa (Cryj1+sHexa), or the Cryj1/sDNA hydrogel was administered i.n. to BALB/c mice at a dose of 50 μg DNA and 10 μg Cryj1/mouse (DNA concentration: 0.1 mM) under anesthesia with pentobarbital. A different set of mice received a subcutaneous (s.c.) injection of Cryj1 at a dose of 10 μg/mouse under anesthesia with isoflurane. The mice were immunized twice on days 0 and 14. At 14 days after the second immunization, the mice were killed and serum, spleen, and NLF were collected. Spleen cells were purified and cultured in the presence of Cryj1 (2.5 μg/ml) in 12-well culture plates for 3 days. The concentration of IL-12p40 in the supernatant was determined as described above. The concentration of IFN-γ in the supernatant was determined by ELISA by using a Mouse IFN gamma ELISA Ready-SET-Go!® (eBioscience, San Diego, CA, USA).

Cryj1-specific antibodies in serum and NLF of mice after immunization

The titers of Cryj1-specific IgG in serum and NLF were measured by ELISA. Briefly, ELISA plates were coated with Cryj1 in PBS overnight at 4°C (2.5 μg/ml Cryj1). After coating, 1000-fold diluted serum samples and non-diluted NLF samples were added to the plates and incubated at 37°C for 2 h. After washing, HRP-labeled anti-mouse IgG (Wako Pure Chemical, Osaka, Japan) was added, and the samples were incubated at 37°C for 1 h. After additional washing, o-phenylenediamine substrate was added, and the OD was measured at 450 nm. Anti-Cryj1 mouse monoclonal antibody (Funakoshi, Tokyo, Japan) was used as a standard for Cryj1-specific IgG.

IgE in serum of mice after nasal immunization

Cryj1, Cryj1 and ssODN (Cryj1+ssODN), Cryj1 and sHexa (Cryj1+sHexa), or the Cryj1/sDNA hydrogel was administered i.n. to BALB/c mice at a dose of 50 μg DNA and 10 μg Cryj1/mouse (DNA concentration: 0.1 mM) under anesthesia with pentobarbital. The mice were immunized three times on days 0, 7 and 14. At 14 days after the third immunization, the mice were killed and serum was collected. The concentration of IgE in serum was determined by ELISA using an OptEIATM set (BD Biosciences).

Histological examination of mouse nose specimens after nasal immunization

PBS, Cryj1, Cryj1 and ssODN (Cryj1+ssODN), Cryj1 and sHexa (Cryj1+sHexa), or the Cryj1/sDNA hydrogel was administered i.n. to BALB/c mice at a dose of 50 μg DNA and 10 μg

Cryj1/mouse (DNA concentration: 0.1 mM) under anesthesia with pentobarbital. Nasal administration was repeated every day for one week. At 24 hours after the last immunization, the mice were killed. The following histological examinations of mouse nose specimens were kindly performed by Professor Shigeharu Fujieda and Dr. Yukinori Kato of Faculty of Medical Science of University of Fukui as previously described [59]. Briefly, facial skin was stripped, heads were severed between the upper and lower jaws, and noses were removed. Fixed in 4% paraformaldehyde for 3 days and decalcified in 0.12 mol/L EDTA solution (pH 6.5) for 7 days at room temperature. After decalcification, specimens were embedded in paraffin, and 4 mm coronal sections were sectioned and stained with hematoxylin and eosin (HE). Also the number of eosinophils in nasal mucosa was counted.

Statistical analysis

Differences were statistically evaluated by one-way analysis of variance (ANOVA) followed by the Tukey-Kramer test for multiple comparisons and Student's t-test for two groups. $P < 0.05$ was considered to be statistically significant.

II-1-3 Results

II-1-3-a. Formation of Cryj1/sDNA hydrogel

Fig. 9 shows typical FE-SEM images of the inner structure of the sDNA hydrogel and Cryj1/sDNA hydrogel. The images indicate that the sDNA hydrogel has a highly ordered structure with plenty of space. The inner structure of Cryj1/sDNA hydrogel was thicker than that of sDNA hydrogel, suggesting that Cryj1 is uniformly bound to the DNA network. The structure of Cryj1/sDNA hydrogel became denser with an increasing DNA concentration.

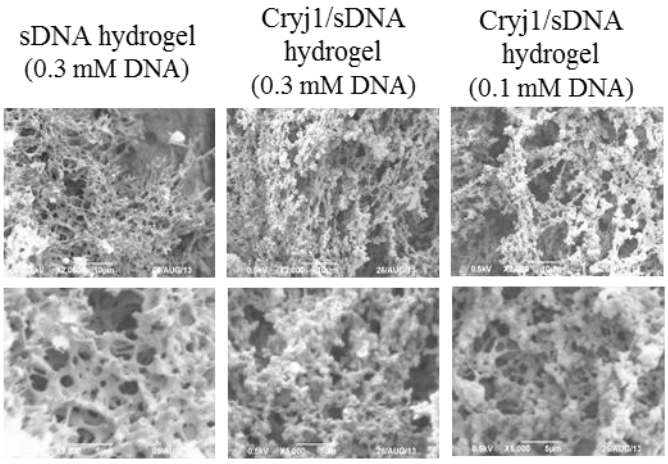

FIGURE 9. FE-SEM images of the inner structure of sDNA hydrogel and Cryj1/sDNA hydrogel. Left, sDNA hydrogel (0.3 mM DNA); center, Cryj1/sDNA hydrogel (0.3 mM DNA); right, Cryj1/sDNA hydrogel (0.1 mM DNA). Images were taken using a field-emission scanning electron microscope at low (×2000, upper panels) and high (×5000, lower panels) magnifications.

II-1-3-b. Sustained release of Cryj1 from sDNA hydrogel

To visualize Cryj1 release, FITC-labeled Cryj1 was encapsulated into sDNA hydrogels prepared at a concentration of 0.1 or 0.3 mM DNA. Fig. 10a shows fluorescence images of the FITC-Cryj1/sDNA hydrogel placed into the upper chamber of the Transwell. The images clearly show that FITC-Cryj1 was slowly released from the sDNA hydrogel. When a 0.3 mM sDNA hydrogel was applied, FITC-Cryj1 remained at the location where the hydrogel was placed for at least 1 h. In contrast, FITC-Cryj1 quickly

diffused away soon after a 0.1 mM sDNA hydrogel was applied. These results suggest that the shape of the 0.3 mM sDNA hydrogel was maintained longer than that of the 0.1 mM sDNA hydrogel. No significant differences in the fluorescence images were observed between the two groups at 6 h or later. The fluorescence intensity of the solution in the lower chamber also showed that FITC-Cryj1 was gradually released from the sDNA hydrogel, whereas it was rapidly released from sHexa solution within 2 h (Fig. 10b). The initial release of Cryj1 from the 0.1 mM sDNA hydrogel was faster than that from the 0.3 mM sDNA hydrogel, but no significant difference between the 0.1 mM and 0.3 mM hydrogels was observed in the release profile at 6 h or later.

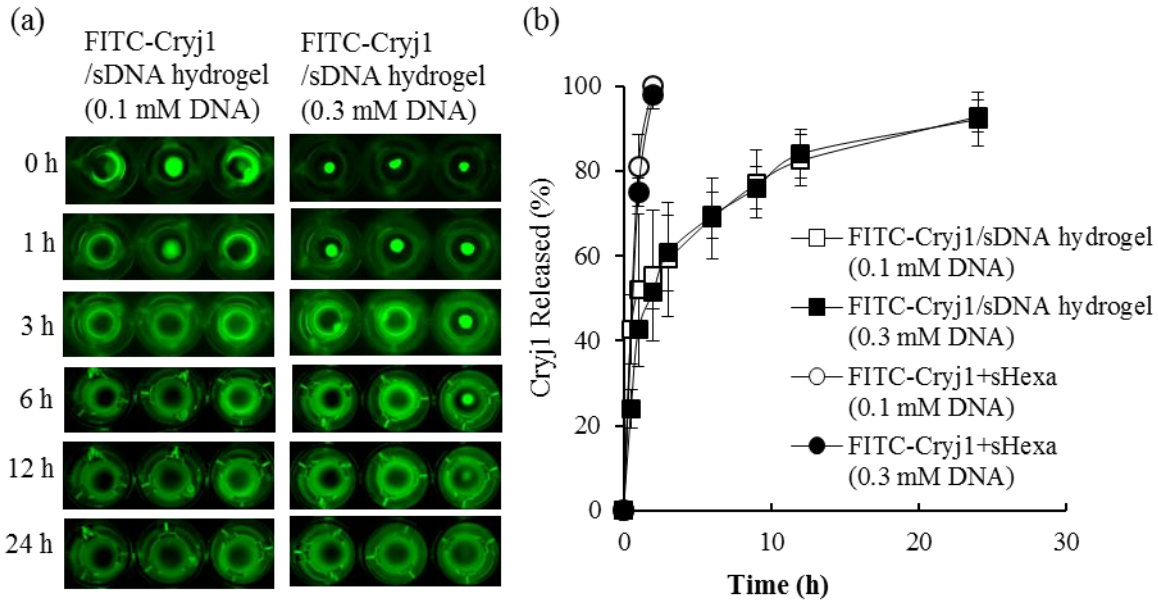

FIGURE 10. Cryj1 release from sDNA hydrogel. FITC-Cryj1 was loaded into the sDNA hydrogel or mixed with sHexa solution at a ratio of 1 μg Cryj1/5 μg DNA, and then placed into the upper chamber of the Transwell (0.4-μm pore size) with the bottom chamber containing PBS, followed by incubation at 37°C. (a) The fluorescence images of the FITC-Cryj1/sDNA hydrogel prepared at DNA concentrations of 0.1 mM (left) and 0.3 mM (right) were photographed at the indicated times. (b) The concentration of FITC-Cryj1 released from 0.1 mM or 0.3 mM sDNA hydrogel and 0.1 or 0.3 mM sHexa solution was measured and plotted against time.

II-1-3-c. IL-12 release from RAW264.7 cells by the Cryj1/sDNA hydrogel

To investigate the effect of sDNA hydrogel formation and Cryj1 loading into the sDNA hydrogel on the production of an innate immune response, IL-12 release from RAW264.7 cells was examined after addition of a variety of components of the sDNA hydrogel with or without Cryj1. Fig. 11 shows the IL-12 concentrations in the supernatant of the RAW264.7 cells at 16 h after addition of Cryj1 (20 μg/ml), DNA (100 μg/ml) or their combination. The IL-12 secretion induced by the Cryj1/sDNA hydrogel was significantly greater ($P < 0.05$) than that induced by Cryj1+ssODN or Cryj1+sHexa. In addition, Cryj1+sHexa induced higher secretion of IL-12 than Cryj1+ssODN. The nsDNA hydrogel with no CpG motifs induced only low IL-12 secretion in the medium. There was no significant difference between sDNA hydrogel and Cryj1+sDNA hydrogel, suggesting that Cryj1 itself hardly has any effect on IL-12 induction.

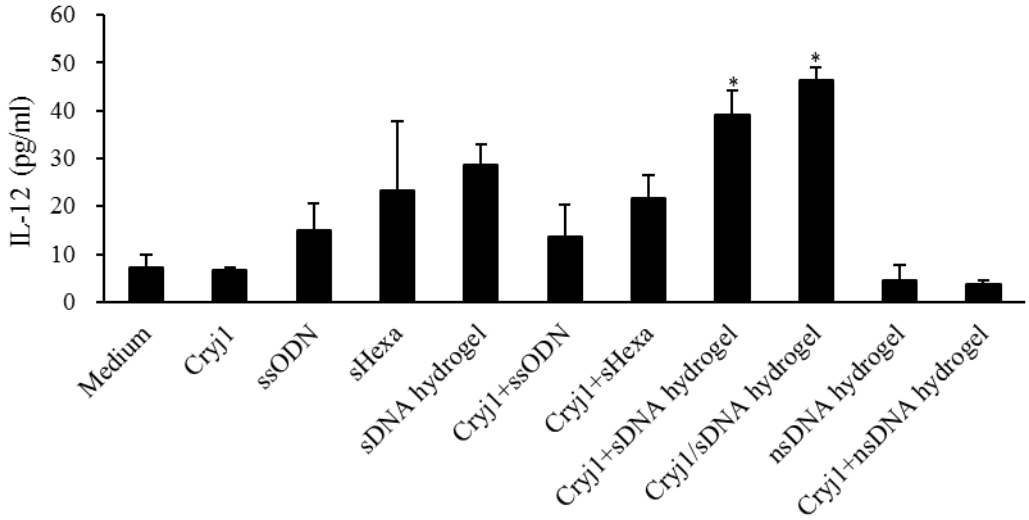

FIGURE 11. IL-12 release from RAW264.7 cells after addition of Cryj1, ssODN, sHexa, sDNA hydrogel, nsDNA hydrogel, their mixture with Cryj1, and Cryj1/sDNA hydrogel at a ratio of 20 μg Cryj1/100 μg DNA. IL-12 in the supernatant was measured after 16 h of incubation with each component. Results are expressed as mean ± SD of three determinations. *P < 0.05, significantly different from the Cryj1+ssODN group.

II-1-3-d. Cellular uptake of FITC-Cryj1 by RAW264.7 cells

Fig. 12 shows the mean fluorescence intensity (MFI) of RAW264.7 cells incubated at 37°C after addition of FITC-Cryj1, FITC-Cryj1+ssODN, FITC-Cryj1+sHexa, FITC-Cryj1+sDNA hydrogel, or FITC-Cryj1/sDNA hydrogel. The MFI of cells incubated with the FITC-Cryj1/sDNA hydrogel was significantly greater ($P < 0.05$) than that incubated with any other samples examined, suggesting that FITC-Cryj1 loading into sDNA hydrogel increase cellular uptake of FITC-Cryj1.

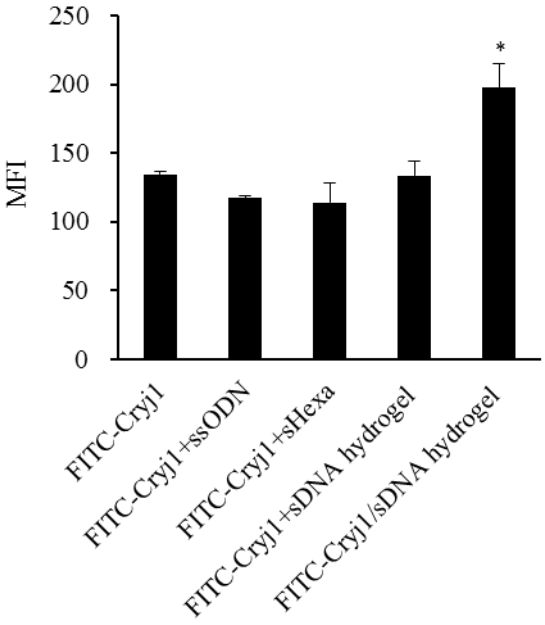

FIGURE 12. Uptake of FITC-Cryj1 by RAW 264.7 cells. RAW264.7 cells were incubated at 37°C for 3 h with FITC-Cryj1, FITC-Cryj1+ssODN, FITC-Cryj1+sHexa, FITC-Cryj1+sDNA hydrogel, or FITC-Cryj1/sDNA hydrogel at concentrations of 20 μg/ml FITC-Cryj1 and 100 μg/ml DNA. The amounts of FITC-Cryj1 associated with cells were measured by flow cytometry. Results are expressed as mean ± SD of four determinations. *P < 0.05, significantly different from all other groups.

II-1-3-e. Distribution and clearance of FITC-Cryj1/sDNA hydrogel after intranasal administration to mice

Fig. 13a shows the amount of FITC-Cryj1 and DNA remaining in the nasal cavity after intranasal administration of FITC-Cryj1+sHexa or the FITC-Cryj1/sDNA hydrogel. In both cases, FITC-Cryj1 and DNA showed similar elimination profiles. The half-life of FITC-Cryj1 and DNA in the nasal cavity was approximately 3-4 h after administration of the FITC-Cryj1/sDNA hydrogel, whereas it was approximately 0.5 h after administration of FITC-Cryj1+sHexa. Fig. 13b shows fluorescence images of mouse heads after intranasal administration of Cryj1+sHexa or the Cryj1/sDNA hydrogel. To visualize DNA, the sHexa and sDNA hydrogel remaining in the cavity were stained with SYBR Gold. This imaging also showed that the sDNA hydrogel remained in the nasal cavity for a longer period of time than sHexa.

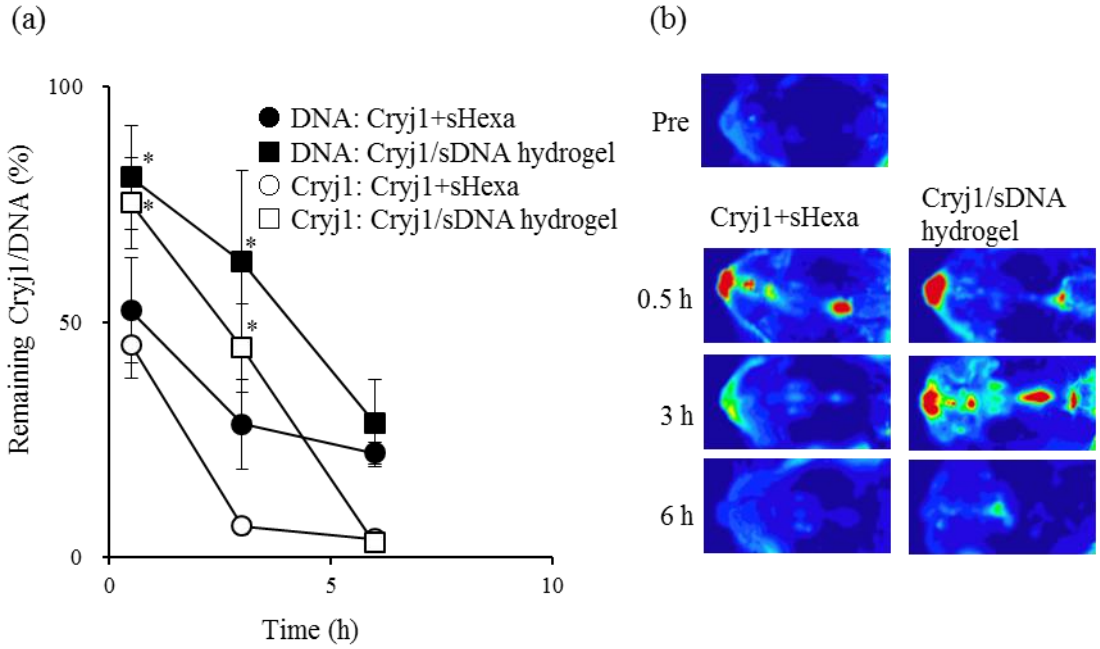

FIGURE 13. Distribution and clearance of FITC-Cryj1/sDNA hydrogel in nasal cavity after nasal administration into mice. (a) FITC-Cryj1+sHexa or FTIC-Cryj1/sDNA hydrogel (50 μg DNA, 10 μg Cryj1/mouse) was intranasally administrated. NLF was collected at the indicated time, and the concentration of DNA and Cryj1 from FITC-Cryj1+sHexa or the FITC-Cryj1/sDNA hydrogel was measured and plotted against time. (b) Cryj1+sHexa (left) or the Cryj1/sDNA hydrogel (right) was intranasally administered after staining of DNA with SYBR Gold (50 μg DNA, 10 μg Cryj1/mouse). Mice were killed at the indicated time and dissected. Then, fluorescence distribution around the nasal mucosa was photographed. As a control, the fluorescence distribution before administration was also photographed (Pre, top).

II-1-3-f. IL-12 production after intranasal administration of sDNA hydrogel to mice

Fig. 14 shows the concentration of IL-12 in the serum and NLF at 6 h after intranasal administration of saline, ssODN or the sDNA hydrogel at a dose of 50 μg/mouse. The level of IL-12 in the serum after administration of sDNA hydrogel was significantly ($P<0.05$) greater than that after administration of ssODN, and a similar trend was observed in the IL-12 level of the NLF. These results suggest that hydrogel formation increases the potency of CpG DNA to induce systemic and mucosal Th1 immune responses.

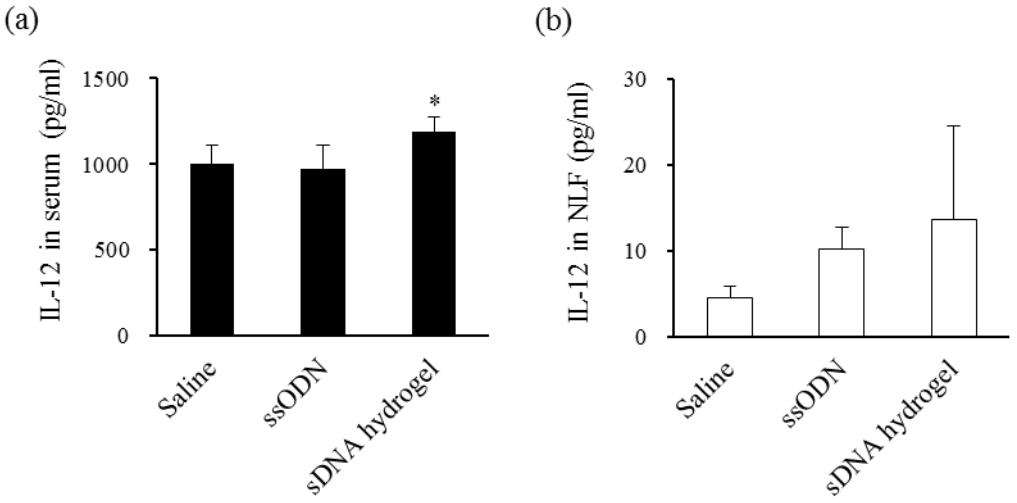

FIGURE 14. IL-12 production after intranasal administration of the sDNA hydrogel to mice. Saline, ssODN, or the sDNA hydrogel was administrated intranasally to mice (50 μg/mouse). At 6 h after injection, serum and NLF were collected to measure the level of IL-12. (a) IL-12 concentration in serum. (b) IL-12 concentration in NLF. Results are expressed as the mean ± SD of five determinations. *P < 0.05, significantly different from the ssODN alone group.

II-1-3-g. Induction of immune response to Cryj1 by intranasal administration of Cryj1/sDNA hydrogel

To investigate the effects of CpG DNA formulation, Cryj1 loading into the hydrogel, and administration route on the inhibition of allergic reactions, the Cryj1-specific Th1immune response and Cryj1-specific antibody levels after immunization were evaluated. Fig. 15a shows the concentration of IL-12 in the supernatant of spleen cells after re-stimulation with Cryj1 for 72 h. The spleen cells from mice immunized with intranasal Cryj1/sDNA hydrogel produced significantly ($P<0.05$) more IL-12 than those from mice treated with subcutaneous Cryj1, intranasal Cryj1, or intranasal Cryj1+ssODN. Fig. 15b shows the concentration of IFN-γ in the supernatant of spleen cells after re-stimulation with Cryj1 for 72 h. The spleen cells from mice immunized with intranasal Cryj1/sDNA hydrogel produced significantly ($P<0.05$) more IFN-γ than those from mice treated with intranasal Cryj1, or intranasal Cryj1+ssODN. No significant difference in IL-12 and IFN-γ secretion from re-stimulated spleen cells was observed among the different administration routes of Cryj1.

Intranasal immunization with the Cryj1/sDNA hydrogel induced a higher level of Cryj1-specific IgG in the serum and a higher level of Cryj1-specific IgG in the NLF compared with intranasal immunization with Cryj1, Cryj1+ssODN, or Cryj1+sHexa (Fig. 15c, d).

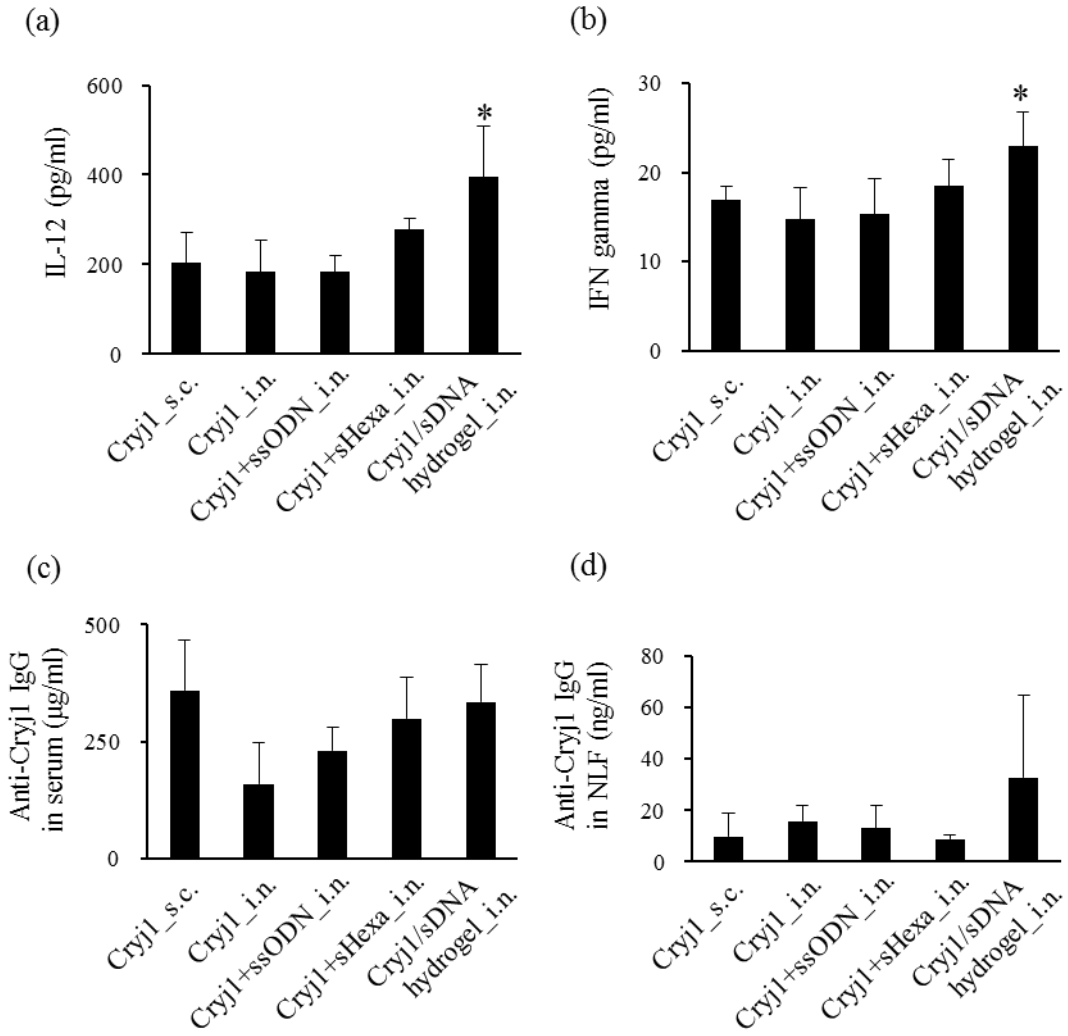

FIGURE 15. Induction of Cryj1-specific immune reactions by intranasal administration of Cryj1/sDNA hydrogel. Mice were immunized on days 0 and 14 with Cryj1 subcutaneously (s.c.), Cryj1 intranasally (i.n.), Cryj1+ssODN i.n., Cryj1+sHexa i.n. or Cryj1/sDNA hydrogel i.n. (50 μg DNA, 10 μg Cryj1/mouse). At 14 days after the last immunization, spleen cells, serum, and NLF were collected. (a) Concentration of IL-12 in the supernatant of spleen cells at 72 h after re-stimulation with Cryj1. (b) Concentration of IFN-γ in the supernatant of spleen cells at 72 h after re-stimulation with Cryj1. (c) Concentration of Cryj1-specific IgG in serum. (d) Concentration of Cryj1-specific IgG in NLF. *$P < 0.05$, significantly different from the Cryj1 only group and Cryj1+ssODN i.n. group.

II-1-3-h. Suppression of Th2 response by intranasal administration of Cryj1/sDNA hydrogel

To investigate the effects of Cryj1 loading into the sDNA hydrogel on the inhibition of allergic sensitivity, serum IgE level after immunization were evaluated as a Th2 response indicator. Fig. 16 shows the concentration of IgE in the serum after immunization. The serum IgE level of Cryj1/sDNA hydrogel group was significantly lower ($P < 0.05$) than that of Cryj1 only group, suggesting that loading of Cryj1 into sDNA hydrogel could attenuate Th2 response, and suppress allergic reaction.

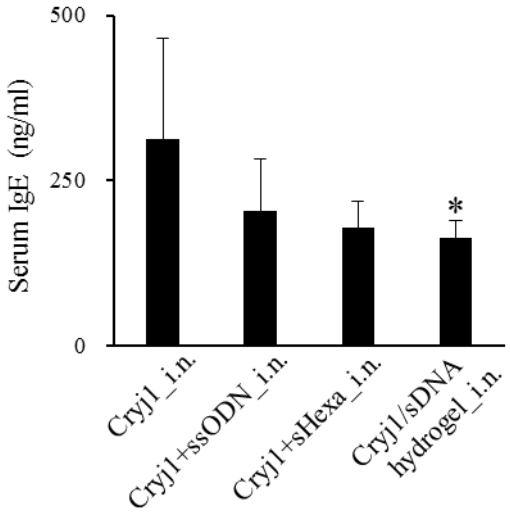

FIGURE 16. Supression of Th2 response by intranasal administration of Cryj1/sDNA hydrogel. Mice were immunized on day 0, 7 and 14 with Cryj1 intranasally (i.n.), Cryj1+ssODN i.n., Cryj1+sHexa i.n. or Cryj1/sDNA hydrogel i.n. (50 μg DNA, 10 μg Cryj1/mouse). At 14 days after the last immunization, serum was collected, and the concentration of IgE in serum was measured. Results are expressed as mean ± SD of six determinations. *P < 0.05, significantly different from the Cryj1 only group.

II-1-3-i. Histological examination of mouse nose specimens after intranasal administration of Cryj1/sDNA hydrogel

To evaluate the effect of Cryj1/sDNA hydrogel by intranasal administration on allergic inflammation of nasal mucosa, histological examination was performed. Fig. 17a shows the hematoxylin and eosin sections of nasal tissues after repeated immunization for one week. Cryj1/sDNA hydrogel group did not show significant multilayered epithelium, globet cell hyperplasia or infiltration of eosinophils in nasal mucosa compared with PBS group. Also there was no significant difference of the number of eosinophils in nasal mucosa (Fig. 17b) between groups, indicating that Cryj1/sDNA hydrogel could be a safe intranasal formulatoin which does not induce allergic inflammation even after repeated nasal immunization.

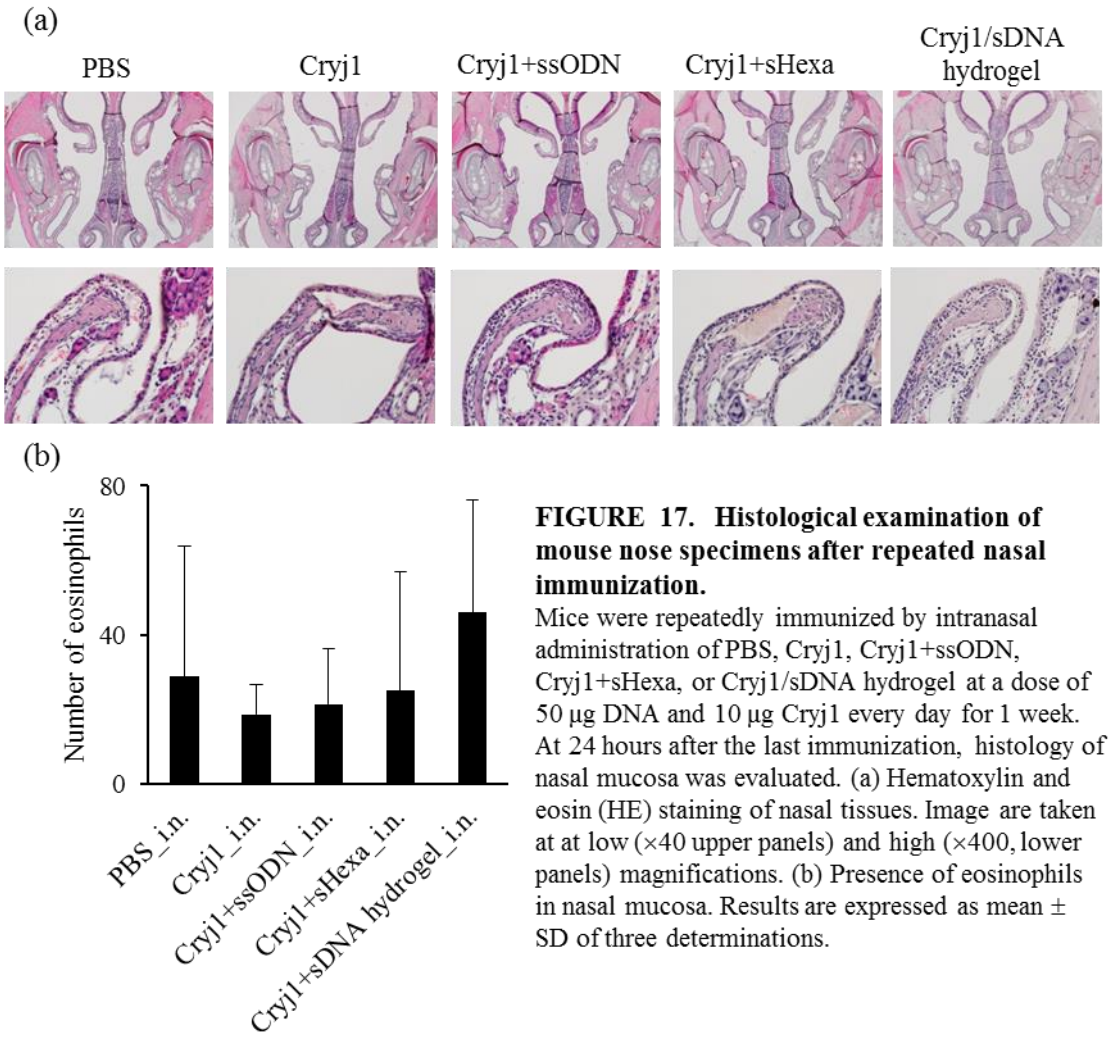

FIGURE 17. Histological examination of mouse nose specimens after repeated nasal immunization.
Mice were repeatedly immunized by intranasal administration of PBS, Cryj1, Cryj1+ssODN, Cryj1+sHexa, or Cryj1/sDNA hydrogel at a dose of 50 μg DNA and 10 μg Cryj1 every day for 1 week. At 24 hours after the last immunization, histology of nasal mucosa was evaluated. (a) Hematoxylin and eosin (HE) staining of nasal tissues. Image are taken at at low (×40 upper panels) and high (×400, lower panels) magnifications. (b) Presence of eosinophils in nasal mucosa. Results are expressed as mean ± SD of three determinations.

II-1-4 Discussion

Understanding of the mechanisms underlying pollen-induced allergic rhinitis has led to the development of vaccines against allergies [60]. Although subcutaneous injection of allergens has traditionally been the main immunotherapy method, several other formulations including sublingual solutions of JCP extracts and sublingual tablets containing grass pollen extracts have been approved in the US, Japan, and other countries [58]. In addition, local intranasal delivery of allergens is another promising method for administration, and several clinical trials have been conducted worldwide [61]. Intranasal immunotherapy could be convenient and ensure patient compliance, although current formulations would induce an insufficient immune response because of rapid clearance and inefficient uptake of the allergen by nasal immune cells [62]. Thus far, CpG DNA has been applied in the intranasal delivery of allergens as an adjuvant for allergic rhinitis immunotherapy to induce an efficient immune response [63], but no attempts have been made to use CpG DNA as a component for a controlled release formation of allergens. Therefore, we examined in this study whether an injectable DNA hydrogel consisting of CpG DNA that we previously developed is useful for intranasal delivery of Cryj1, the typical allergen of JCP.

As demonstrated in previous study of my laboratory using ovalbumin as a cargo [15], Cryj1 was slowly released from the DNA hydrogel not only under in vitro conditions but also in the nasal cavity of

mice (Figs. 10, 13). Because sustained release of antigens is well known to effectively induce antigen-specific immune responses [64, 65], this slow release of Cryj1 from sDNA hydrogel should result in the induction of a high level of Cryj1-specific immune responses (Fig. 15).

One of unique findings for nanostructured CpG DNA is that the immunostimulatory activity of CpG DNA is dependent on the structural complexity of the DNA, which should be at least partly related to increased cellular uptake of CpG DNA [50, 66, 67]. The higher activity of the sDNA hydrogel, which consists of two sets of hexapodna, compared to sHexa (Figs. 11, 14) clearly indicates that multiple units of hexapodna would be efficiently taken by cells and recognized by the immune cells when the sDNA hydrogel is used. Efficient cellular uptake of DNA hydrogel is supposed to result in increased uptake of Cryj1 when added to RAW264.7 cells as Cryj1/sDNA hydrogel (Fig. 12). The importance of the immunostimulatory CpG motif in the immune responses was also confirmed by the IL-12 release from RAW264.7 cells (Fig. 11), which was comparable with the previous results for a DNA hydrogel containing OVA [15]. Therefore, the efficient induction of Cryj1-sepcific immune response by the Cryj1/sDNA hydrogel (Fig. 15) and the efficient suppression of Th2 response (Fig. 16) results from (1) the sustained release of Cryj1 from the hydrogel and (2) the high immunostimulatory activity of the sDNA hydrogel relative to sHexa. Cryj1-specific IgG after intranasal immunization (Fig. 15c, d) did not show significant differences among the groups, although it tended to increase by loading Cryj1 into sDNA hydrogel. This could be explained by considering that the immunization increased only some IgG subtypes.

Nasal sprays are a patient-friendly device for drug administration to the nasal cavity. To increase the retention of pharmaceutical agents within the cavity, hydrogels are used for the intranasal delivery. Although this approach is promising, the administration of hydrogels is not suitable for the spread of the sprayed materials within the cavity [68]. Substrates that form gels upon changes in environmental factors, such as temperature changes, would solve this problem [69]. In the present study, we administered a DNA hydrogel prepared in vitro prior to administration to mice. However, the self-gelling property of the DNA hydrogel enables us to deliver the components, i.e., hexapodna in the present case, as a solution and then to obtain the DNA hydrogel by spontaneous hybridization of the components within the nasal cavity. This property will be beneficial for DNA hydrogels prepared using self-gelling nucleic acids.

II-1-5 Conclusion

I demonstrated that a CpG motif-containing sDNA hydrogel loaded with Cryj1 is useful to induce effective immune responses specific to Cryj1 by intranasal administration. Our results also indicate that the sustained release of Cryj1 from the sDNA hydrogel and the efficient immune stimulation by the sDNA hydrogel are the major two factors underlying the Cryj1-specific immune responses. These findings introduce the application of DNA hydrogels as a mucosal delivery system for shorter immunotherapy with a lower burden.

Chapter II

Section 2

Improvement of sustained release system of antigen from immunostimulatory DNA hydrogel

II-2-1 Introduction

Section 1 of Chapter II and other previous studies have demonstrated that CpG motif-containing immunostimulatory DNA hydrogel (sDNA hydrogel) is a useful antigen delivery carrier [15, 70]. The efficient induction of antigen specific immune response was at least partially due to the sustained release of antigen from sDNA hydrogel. However, the half-life of the antigen release from sDNA hydrogel was less than 3 h under in vitro conditions. Particularly, negatively charged antigens will hardly interact with DNA, leading to their rapid release from sDNA hydrogel. Considering the well-known fact that sustained release of antigens effectively induces antigen-specific immune response [64, 65, 71, 72], there seems to be potential to improve the potency of sDNA hydrogel by increasing the duration of antigen release. To investigate this potential, in my laboratory, OVA, a negatively charged antigen, was cationized to electrostatically interact with DNA. The cationized OVA was slowly released from sDNA hydrogel, and intratumoral injections of this formulation was more potent than noncationized OVA/sDNA hydrogel in suppressing the growth of EG7-OVA tumors in mice [73].

Prolonged TLR signals could be the main warning signal to the immune system not to shut down a response but to continue with the expansion of immune effector cells via sustained release of proinflammatory cytokines [74, 75]. Slow release of TLR ligands including CpG DNA showed enhanced antigen specific immune response in mice [75, 76].

It seems to be useful to optimize the function of sDNA hydrogel itself for sustained release of not only antigen but also CpG DNA, which enables application for various types of antigens and drugs regardless of its electric charge. The use of electrostatic interaction between oppositely charged polymers is a major approach to obtain reversible polyelectrolyte complexes [77, 78]. For example, chitosan, a cationic polymer, interacted with a polyanionic tripolyphosphate (TPP) via electrostatic force and led to ionic gelation, although its usage in drug delivery is limited because of its poor mechanical strength [78]. In addition, it was demonstrated that electrostatic interaction between chitosan and plasmid DNA (pDNA) resulted in the formation of polyelectric complexes, and improved the transfection efficiency of pDNA by protection of DNA from nuclease degradation [79]. Therefore, cationic polymers are expected to electrostatically interact with sDNA hydrogel to modify its function.

Based on these considerations, in Section 2 of Chapter II, I aimed to stabilize sDNA hydrogel by electrostatic interaction between cationic polymer and DNA to improve sustained release of antigen and CpG DNA. A major natural biodegradable polysaccharide chitosan was selected as a cationic polymer, and the effect of chitosan on physicochemical properties on DNA hydrogel was examined. Chitosan-mixed

sDNA hydrogel was loaded with OVA, a model antigen, and then the properties of the chitosan-mixed sDNA hydrogel on sustained release and induction of antigen specific immune response were investigated.

II-2-2 Materials and Methods

Chemicals

Ultrapure medical grade water-soluble chitosan glutamate (PROTASAN UP G213) was purchased from FMC biopolymer (Philadelphia, PA, USA), which has been shown to be nontoxic in vitro and in vivo [80, 81]. Polyethylene glycol (POLYOX WSR 303) was obtained from Dow chemical company (MI, USA). Sodium alginate (sodium alginate 300-400) was purchased from Wako Pure Chemical (Osaka, Japan). All other chemicals were of the highest grade available and used without further purification.

Animals

Male C57BL6 mice (5 weeks old) were purchased from Japan SLC, Inc. (Shizuoka, Japan). Animals were maintained under conventional housing conditions. All animal experiments were approved by the Animal Experimentation Committee of the Graduate School of Pharmaceutical Sciences, Kyoto University.

Preparation of DNA hydrogel, polymer-mixed DNA hydrogel

All phosphodiester oligodeoxynucleotides (ODNs) were purchased from Integrated DNA Technologies, Inc. (Coralville, IA, USA). The hexapodna and DNA hydrogel was designed and prepared using the ODNs as reported in previous study of my laboratory as described in Section 1 of Chapter II [15]. Briefly, three types of immunostimulatory hexapodna (sHexa) with potent CpG motifs (sHexa-1, sHexa-2 and sHexa-3), and two types of non-immunostimulatory hexapodna (nsHexa) with no CpG motifs were prepared (nsHexa-1 and nsHexa-2). Immunostimulatory and non-immunostimulatory DNA hydrogels (sDNA hydrogel and nsDNA hydrogel, respectively) were obtained by mixing equimolar amounts of sHexa-1 and sHexa-2 or nsHexa-1 and nsHexa-2, respectively, at an initial concentration of 0.1 or 0.3 mM DNA (7 μg/μl DNA or 22 μg/μl DNA, respectively). sHexa solution was prepared by mixing sHexa-1 and sHexa-3.

To prepare polymer-mixed DNA hydrogels, three different polymer solutions, chitosan glutamate solution, polyethylene glycol solution and sodium alginate solution were prepared in advance at a concentration of 20 μg/μl in TE buffer containing 150mM NaCl. The viscosity and Zeta potential of each polymer solution at the final concentration in polymer-mixed DNA hydrogel was measured using a viscometer (RheoSense, Micro VISC, San Ramon, CA, USA) and a Zetasizer (ZEN3600, Malvern Instruments, Worcestershire, UK). The polymer solutions were mixed with sHexa-1 or nsHexa-1 in BD Ultra-fine II, U-100, 0.5 ml, 30 G × 5/16 inch 29G syringe (Becton Dickinson, CA USA) followed by mixing with sHexa-2 or nsHexa-2. Then DNA hydrogels mixed with chitosan glutamate (Chitosan-DNA hydrogel), with polyethylene glycol (PEG-DNA hydrogel) or with sodium alginate (Alg-DNA hydrogel) were obtained. The concentration of polymer in DNA hydrogel was set at 7 μg/μl or 15 μg/μl. Hydrogel formation was briefly confirmed by 6% PAGE as previously reported [15].

Preparation of DNA hydrogel and Chitosan-DNA hydrogel loaded with OVA

To prepare the OVA-loaded sDNA hydrogel (OVA/sDNA hydrogel) and OVA loaded Chitosan-sDNA hydrogel (OVA/Chitosan-sDNA hydrogel), OVA was added to sHexa-1 followed by

mixing with chitosan glutamate solution and sHexa-2 in a 29-gauge syringe. Hydrogel formation was briefly confirmed by adding a solution containing blue dextran (Sigma-Aldrich), which does not instantly diffuse into hydrogels [15].

DNA release from DNA hydrogel in vitro

sDNA hydrogel, Chitosan-sDNA hydrogel, PEG-sDNA hydrogel and Alg-sDNA hydrogel were prepared at the concentration of 22 μg DNA/μl, 7 μg polymer/μl (the polymer to DNA ratio of 0.3) or 7 μg DNA/μl, 15 μg polymer/μl (the polymer to DNA ratio of 2). Then, 10 μl of the preparations were placed into the upper chamber of a Transwell (Product#3460, 0.4-μm pore size; Corning Inc., Corning, NY, USA), and 1000 μl of PBS was added into the bottom chamber, followed by incubation at 37°C. At predetermined time points, DNA concentration in the bottom chamber was measured at 260 nm by NanoDrop™ 2000 (Thermo Scientific, Waltham, MA, USA)

Degradation of DNA hydrogel in the presence of DNase

sDNA hydrogel and Chitosan-sDNA hydrogel were prepared at the concentration of 22 μg DNA/μl, 7 μg chitosan/μl (the chitosan to DNA ratio of 0.3). Then, 10 μl of the preparations were incubated at 37°C in 100 μl solution containing DNase I (0.002 U/μg of DNA) in a 0.5 ml microcentrifuge tube. At predetermined time points, supernatant was removed, and the amount of remaining DNA was evaluated by measuring absorbance of 260 nm at 95°C.

Measurement of viscoelastic properties of DNA hydrogel

nsDNA hydrogel and Chitosan-nsDNA hydrogel were prepared at the concentration of 22 μg DNA/μl, 7 μg chitosan/μl (the chitosan to DNA ratio of 0.3). The rheological behavior of the preparations was kindly examined by Professor Hiroshi Watanabe of Chemical Research Institute of Kyoto University using a laboratory rheometer (ARES; Rheometric Scientific currently TA Instruments, USA) at room temperature (~ 25°C). A parallel-plate fixture with the diameter of 8.0 mm was used for oscillatory and steady flow tests, following a standard protocol of rheological test [15].

Measurement of T1 relaxation time of water in DNA hydrogel

sDNA hydrogel and Chitosan-sDNA hydrogel were prepared at the concentration of 22 μg/μl DNA, 7 μg/μl chitosan (the chitosan to DNA ratio of 0.3). The measurement was kindly performed by Professor Yoshinori Onuki of Toyama University using a 9.4 T vertical MRI scanner (Varian, Palo Alto, CA, USA). Briefly, T1 relaxation time was measured using a Varian NMR system (Varian Technologies Japan Ltd., Tokyo, Japan). In addition, to visualize the water state in DNA hydrogels, T1 mapping was carried out as previously described [82].

OVA release from DNA hydrogel in vitro

OVA was labeled with fluorescein isothiocyanate (FITC; fluorescein isothiocyanate isomer 1, Sigma-Aldrich, St. Louis, MO, USA) to obtain FITC-OVA. FITC-OVA-loaded sDNA hydrogel (FITC-OVA/sDNA hydrogel) and OVA loaded Chitosan-sDNA hydrogel (FITC-OVA/Chitosan-sDNA hydrogel) were prepared at the concentration of 2.2 μg OVA/μl. The concentration of DNA and chitosan was 22 μg DNA/μl, 7 μg chitosan/μl (the chitosan to DNA ratio of 0.3) or 7 μg DNA/μl, 15 μg chitosan/μl (the chitosan to DNA ratio of 2). Aliquots (10 μl) of the preparations were placed into the upper chamber of

a Transwell (Product#3460, 0.4-μm pore size; Corning Inc., Corning, NY, USA), and 1000 μl of PBS was added into the bottom chamber, CA, USA).

Immunization of mice

OVA, OVA/sDNA hydrogel and OVA/Chitosan-sDNA hydrogel were prepared at the concentration of 2.2 μg OVA/μl. The concentration of DNA and chitosan was 22 μg DNA/μl, 7 μg chitosan/μl (the chitosan to DNA ratio of 0.3) or 7 μg DNA/μl, 15 μg chitosan/μl (the chitosan to DNA ratio of 2). Under isoflurane-induced anesthesia, C57BL/6 mice were intradermally injected with 10 μl of each preparation. Mice were immunized two times on days 0 and 14. At 14 days after the last immunization, mice were euthanized with isoflurane, and serum was collected. Serum samples were stored at −80 °C until measurement.

Measurement of OVA-specific antibody

Serum samples were serially diluted to measure the OVA-specific total IgG levels by ELISA as previously described [83].

Statistical analysis

Differences were statistically evaluated by one-way analysis of variance (ANOVA) followed by the Tukey-Kramer test for multiple comparisons and Student's t-test for two groups. $P < 0.05$ was considered to be statistically significant.

II-2-3 Results

II-2-3-a. DNA release from Chitosan-sDNA hydrogel

To investigate the effect of electrostatic interaction between polymer and DNA, the release profile of DNA from sDNA hydrogel, Chitosan-sDNA hydrogel, Alg-sDNA hydrogel and PEG-sDNA hydrogel was evaluated (Fig. 18a). The charge of each polymer in the same buffer as the tested sDNA hydrogel was 13 mV for chitosan, 0 mV for PEG and -40 mV for Alg. The viscosity of each polymer solution at the same concentration as the tested sDNA hydrogel was similar among the samples (7.7 mPa for chitosan, 6.9 mPa for Alg and 11.6 mPa for PEG). The release of DNA from Chitosan-sDNA hydrogel was significantly slower than all the other groups especially for the first several hours of incubation, whereas that from Alg-sDNA hydrogel and PEG-sDNA hydrogel was comparable to that from sDNA hydrogel. In addition, 100% of DNA was rapidly released from the mixture of sHexa and chitosan (Chitosan-sHexa) within two hours (data not shown). These results indicate that chitosan electrostatically interacts with sDNA hydrogel to stabilize the sDNA hydrogel. The effect of the ratio of chitosan on DNA release profile was also investigated (Fig. 18b). DNA release became slower when the chitosan concentration increased.

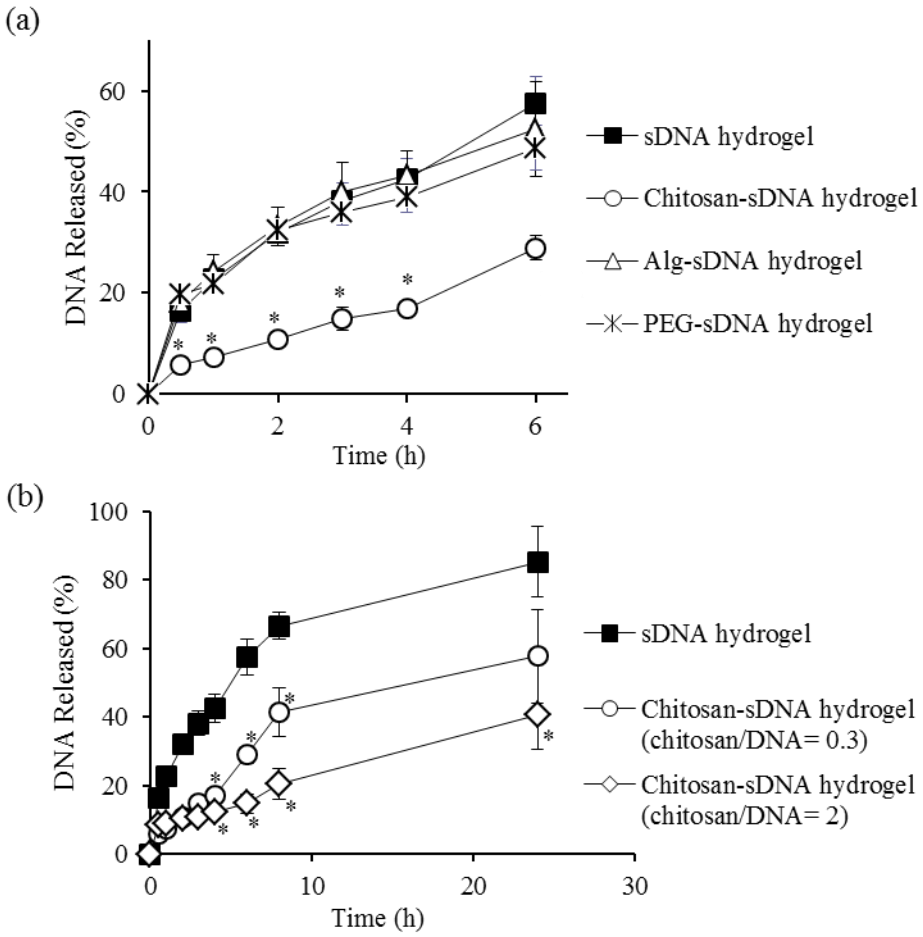

FIGURE 18. DNA release from sDNA hydrogel and polymer-mixed sDNA hydrogels. sDNA hydrogel, Chitosan-sDNA hydrogel, Alg-sDNA hydrogel and PEG-sDNA hydrogel was placed into the upper chamber of the Transwell (0.4-μm pore size) with the bottom chamber containing PBS, followed by incubation at 37℃. The concentration of released DNA was measured and plotted against time. (a) Release profile of DNA from sDNA hydrogel and polymer-mixed sDNA hydrogel (22 μg DNA/μl , 7 μg polymer/μl, the polymer to DNA ratio of 0.3). (b) The Release profile of DNA from sDNA hydrogel and Chitosan-sDNA hydrogel at the different ratio of chitosan. Results are expressed as mean ± SD of three determinations. *P < 0.05, significantly different from sDNA hydrogel.

II-2-3-b. Degradation of Chitosan-sDNA hydrogel in the presence of DNase

Fig. 19 shows the degradation of sDNA hydrogel and Chitosan-sDNA hydrogel in buffer solution containing DNase I. Chitosan-sDNA hydrogel was much more resistant to DNase than sDNA hydrogel, suggesting that chitosan protects DNA hydrogel from degradation by DNase.

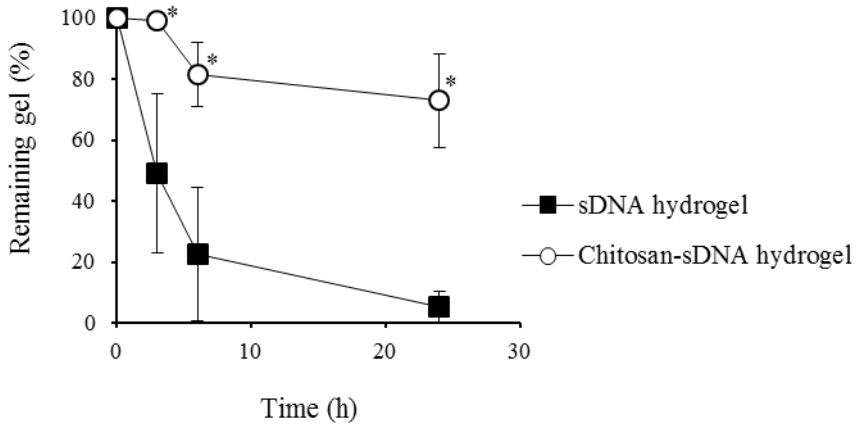

FIGURE 19. Degradation of sDNA hydrogel and Chitosan-sDNA hydrogel in the presence of DNase. sDNA hydrogel and Chitosan-sDNA hydrogel (22 μg DNA/μl, 7 μg chitosan/μl, the chitosan to DNA ratio of 0.3) were incubated at 37 ℃ in the buffer solution containing DNase I (0.002 U/μg of DNA). Results are expressed as mean ± SD of three determinations. *P < 0.05, significantly different from sDNA hydrogel.

II-2-3-c. The viscoelastic property of Chitosan-DNA hydrogel

The viscoelastic property of the DNA hydrogel and Chitosan-DNA hydrogel was examined using a rheometer. Fig. 20 a-b show the storage modulus of DNA hydrogel and Chitosan-DNA hydrogel, respectively, under sinusoidal strain of various amplitudes (γ_0). Storage modulus of DNA hydrogel at a sinusoidal strain of 1 % was 961 Pa and that of Chitosan-DNA hydrogel was 1,360 Pa. Chitosan-DNA hydrogel showed a higher storage modulus under any strain than DNA hydrogel. Fig. 20 c-d show the stress $\sigma^+(t)$ of the samples at a time after start-up of the flow. Chitosan-DNA hydrogel showed a higher stress $\sigma^+(t)$ compared with DNA hydrogel, although the stress decreased under high amplitude. These results indicate that Chitosan-DNA hydrogel retains the elastic property as an injectable DNA hydrogel and also chitosan-DNA hydrogel has more solid-like features compared with DNA hydrogel.

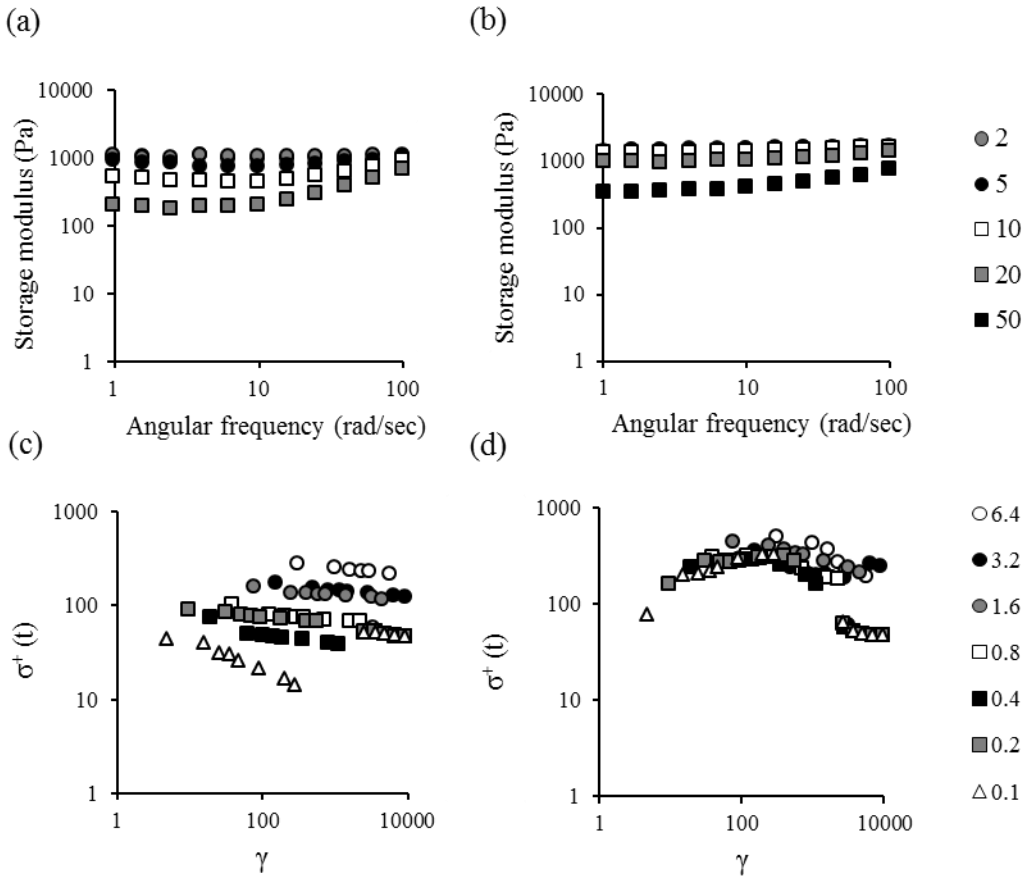

FIGURE 20. Rheological characterization of DNA hydrogel and Chitosan-DNA hydrogel. Rheological characterization of DNA hydrogel and Chitosan-DNA hydrogel hydrogel (22 μg DNA/μl, 7 μg chitosan/μl, the chitosan to DNA ratio of 0.3) at room temperature were evaluated. (a,b) Storage modulus (G') was measured for sinusoidal strain at various angular frequencies (ω) and with the amplitude (γ_0) as indicated. (c,d) Time evolution of the shear stress σ^+ (t) was measured after start-up of shear flow at constant rates (κ) as indicated. The σ^+ (t) are plotted against the strain, $\gamma = \kappa t$. (a, c) DNA hydrogel (b,d) Chitosan-DNA hydrogel.

II-2-3-d. Water states in Chitosan-sDNA hydrogel

From the result that water content of DNA hydrogel at the concentration of 22 μg DNA/μl was 97.8 w/v% [15], the gel properties are expected to be controlled by the state of the water. To investigate the effect of chitosan on water state of sDNA hydrogel, T1 relaxation time of water in DNA hydrogels was evaluated using magnetic resonance (MR) imaging. T1 mapping (Fig. 21a) visualized the water state. Both of sDNA hydrogel and Chitosan-sDNA hydrogel showed uniform decrease of T1 relaxation time compared with water. Measured T1 relaxation time of Chitosan-sDNA hydrogel was significantly shorter than that of sDNA hydrogel (Fig. 21b), suggesting that the Chitosan-sDNA hydrogel has more bound water inside of the hydrogel compared with sDNA hydrogel and the motion of water is restricted. The result agrees with the results of viscoelastic property (Fig. 20).

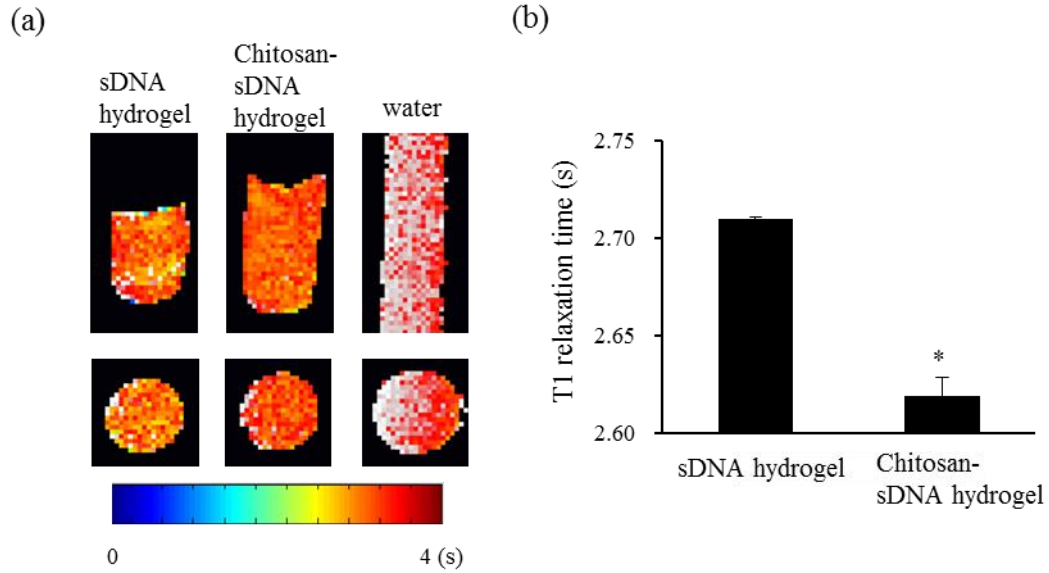

FIGURE 21. Water state in sDNA hydrogel and Chitosan-sDNA hydrogels. Water state in sDNA hydrogel, Chitosan-sDNA hydrogel (22 μg DNA/μl, 7 μg chitosan/μl, the chitosan to DNA ratio of 0.3) were evaluated using a 9.4 T vertical MRI scanner. (a) T1 mapping for sDNA hydrogel, Chitosan-sDNA hydrogel and water. (b) T1 relaxation time measured using a Varian NMR system. Results are expressed as mean ± SD of three determinations. *P < 0.05.

II-2-3-e. Improved sustained release of OVA from Chitosan-sDNA hydrogel

To investigate the sustained release property of antigen from Chitosan-sDNA hydrogel, FITC-labeled OVA was encapsulated into sDNA hydrogel and Chitosan-sDNA hydrogel. Fig. 22a shows the release profile of OVA. Chitosan-sDNA hydrogel prevented the initial burst of OVA, and showed significantly slower release of OVA compared with sDNA hydrogel. OVA/Chitosan-sDNA hydrogel at the concentration of 7 μg DNA/μl showed significantly slower release of OVA compared with OVA/sDNA hydrogel of 22μg DNA/μl. Fig 22b shows fluorescence images of the FITC-OVA/sDNA hydrogel and FITC-OVA/Chitosan-sDNA hydrogel placed into the upper chamber of the Transwell. The images clearly showed that FITC-OVA was much slowly released from Chitosan-sDNA hydrogel compared with sDNA hydrogel.

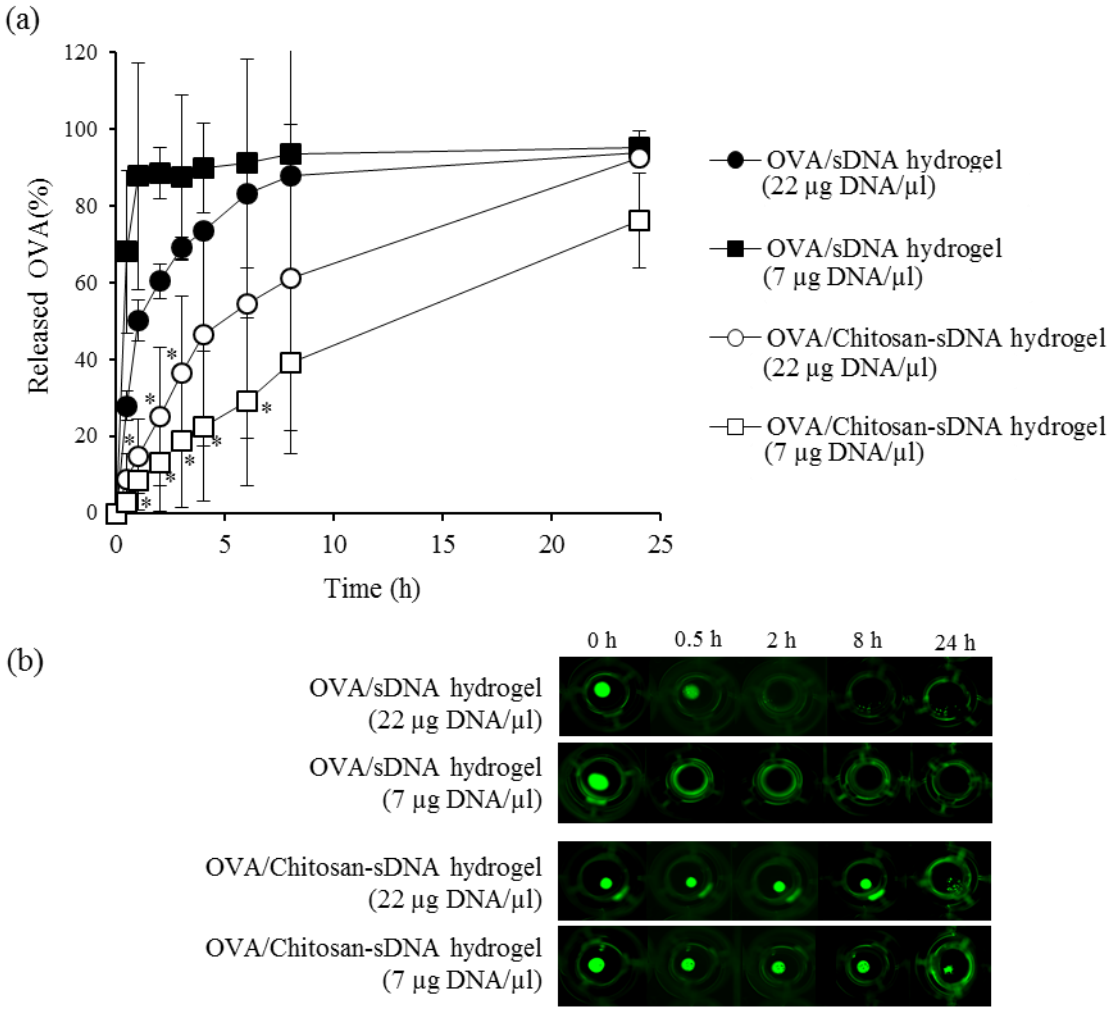

FIGURE 22. OVA release from sDNA hydrogel. FITC-OVA was loaded into the sDNA hydrogel or Chitosan-sDNA hydrogel at the concentration of 2.2 μg OVA/μl. The concentration of DNA and chitosan was 22 μg DNA/μl, 7 μg chitosan/μl (the chitosan to DNA ratio of 0.3) or 7 μg DNA/μl, 15 μg chitosan/μl (the chitosan to DNA ratio of 2). 10μl of preparations were placed into the upper chamber of a Transwell followed by incubation at 37°C. (a) The concentration of FITC-OVA released from sDNA hydrogel or Chitosan-sDNA hydrogel was measured and plotted against time. (b) The fluorescence images of the FITC-OVA/sDNA hydrogel or FITC-OVA/Chitosan-sDNA hydrogel were photographed at the indicated times. Results are expressed as mean ± SD of three determinations. *P < 0.05 vs sDNA hydrogel group.

II-2-3-f. Induction of OVA-specific immune reaction by OVA/Chitosan-sDNA hydrogel

Fig. 23 shows OVA-specific IgG in serum induced after twice immunization. OVA/Chitosan-sDNA hydrogels induced significantly higher OVA-specific IgG than OVA/sDNA hydrogel. There was a trend that OVA-specific IgG level was correlated with sustained release property (Fig. 22), suggesting that improvement of sustained release contributed to the potent adjuvant activity of Chitosan-sDNA hydrogel.

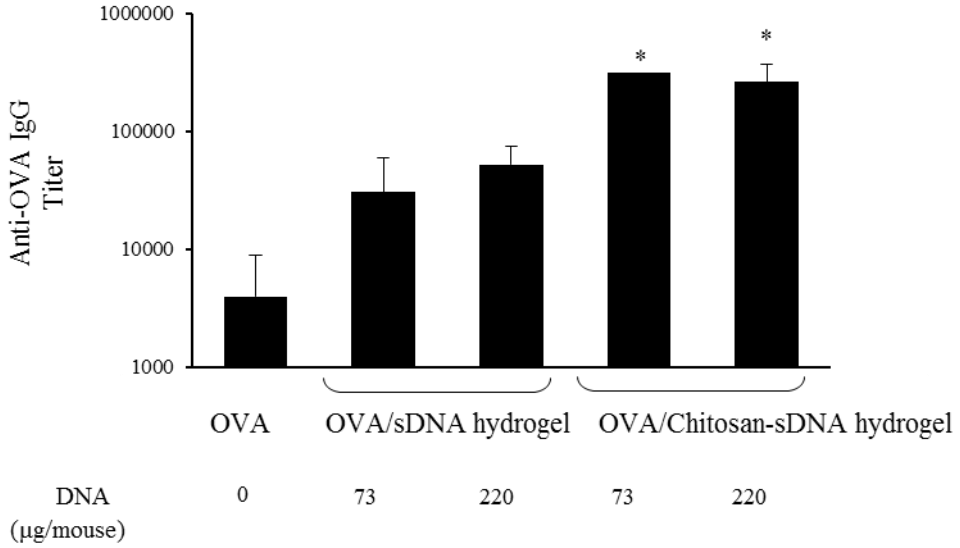

FIGURE 23. Induction of OVA-specific immune reaction by intradermal administration of OVA/Chitosan-sDNAhydrogel. Mice were immunized on days 0 and 14 with OVA, OVA/sDNA hydrogel or OVA/Chitosan-sDNA hydrogel (22 μg OVA/mouse, 10 μl of sample/mouse). The concentration of DNA and chitosan was 22 μg DNA/μl, 7 μg chitosan/μl (the chitosan to DNA ratio of 0.3) or 7 μg DNA/μl, 15 μg chitosan/μl (the chitosan to DNA ratio of 2). At 14 days after the last immunization, serum was collected and concentration of OVA-specific IgG in serum was measured by ELISA. Results are expressed as mean ± SD of four determinations. *P < 0.05, significantly different from the OVA/sDNA hydrogel groups.

II-2-4 Discussion

The slower antigen release from Chitosan-sDNA hydrogel could result from at least two mechanisms. The first is restricted diffusion of antigen in the sDNA hydrogel because of restricted water motion as indicated by increased storage modulus (Fig. 20) and increased bound water (Fig. 21). The second is prolonged dissolution of sDNA hydrogel. This can be explained by stabilized sDNA hydrogel in the solution with or without DNase (Fig. 18, 19), which agree with previous studies reporting that chitosan improved the stability of pDNA against nuclease degradation [79, 85].

The effective induction of antigen specific immune responses by Chitosan-sDNA hydrogel (Fig.22, 23) could reduce the amount of CpG DNA. This is a big benefit of chitosan-sDNA hydrogel compared with sDNA hydrogel not only for antigen specific immune response but also for cost effectiveness. Particularly, vaccine cost is an important factor for economic benefit, because low material cost results in distribution in low-and middle-income countries [86].

Chitosan is a widely investigated material for DDS. However, to the best of my knowledge, Chitosan-sDNA hydrogel is the first attempt and achievement to form hydrogels consisting of DNA and chitosan. Chitosan-sDNA hydrogel has a great advantage as drug delivery carriers for immunotherapy over previously reported chitosan based DDS, because of its potential of sustained delivery of immunostimulatory signals as well as antigen. In the research area of chitosan based DDS, various formulation including micro- or nanoparticle and hydrogels were prepared through several steps of operations, for example emulsion cross-linking, coacervation, spray-dray or chemical cross-linking [77, 78, 84]. Chitosan-sDNA hydrogel was prepared by a simple one-step mixing in syringe without the use of any

organic solvent or reactive agents, alleviating the concern about safety in the body, which is another great attractiveness of Chitosan-sDNA hydrogel as delivery carriers.

One concern involving chitosan-sDNA hydrogel is that it is difficult to be administered using micropipette as conducted in Section1 of Chapter II because of its high storage modulus (Fig. 20), although there is no problem with syringe. For its future nasal application, a safe delivery device to spray it into the nasal cavity needs to be developed. Another concern is that the formation of polyionic complex is affected by the ratio of chitosan to DNA and other preparation conditions, which should be optimized for further development as delivery carriers.

I demonstrated that Chitosan-sDNA hydrogel is a useful DDS carrier for antigens which continuously delivers both immunostimulatory signals and antigens. The component of Chitosan-DNA hydrogel is easy of synthesis on a large scale, biodegradable and low-cost [12, 77, 78, 84], suggesting that Chitosan-sDNA hydrogel could be a realistic formulation for clinical application. Other than vaccine, cancer chemo/immunotherapy using CpG DNA as reported previously [50, 87] could be one of therapeutic applications in the future research.

II-2-5 Conclusion

I have demonstrated that sustained release of antigen from sDNA hydrogel can be improved through electrostatic interaction between DNA and chitosan, and intradermal injection of Chitosan-sDNA hydrogel loaded with antigen induced antigen specific immune response more effectively than the antigen-loaded sDNA hydrogel without chitosan. These findings have implications for optimal immunotherapy based on immunostimulatory DNA hydrogel.

Summary

The aim of this thesis was to develop DDS based on immunostimulatory motif containing DNA (CpG DNA) to deliver drug or antigen and to investigate the potential of CpG DNA as DDS carriers. The main findings from each chapter are summarized as follows.

I. Development of anticancer drug delivery system based on immunostimulatory-motif containing plasmid DNA

To achieve delivery of doxorubicin (DXR), a very commonly used anticancer agent, to tumor tissues, plasmid DNA (pDNA) was intercalated with DXR to obtain a pDNA/DXR complex. The cytotoxic effects of DXR, pDNA and their complex were examined in colon26/Luc cells, a murine adenocarcinoma clone stably expressing firefly luciferase, co-cultured with RAW264.7 murine macrophage-like cells. Both CpG motif-containing pDNA (CpG pDNA) and DXR significantly inhibited the proliferation of colon26/Luc cells, but their complex was the most effective among those examined. Non-CpG pDNA was less effective than CpG pDNA. When injected into mice bearing hepatic metastases of colon26/Luc cells, the CpG pDNA/DXR complex produced a significant level of IL-12 in the serum and liver. The amount of DXR delivered to tumor tissues in the liver was greater when DXR was injected as a CpG pDNA/DXR complex than as free DXR. The CpG pDNA/DXR complex effectively inhibited the proliferation of colon26/Luc cells in the liver compared with free DXR, CpG pDNA, or non-CpG pDNA/DXR complex. These results indicate that CpG pDNA is an effective polymer that inhibits tumor growth by delivering both a proinflammatory signal and anticancer agent to tumor tissues.

II. Development of antigen delivery system based on immunostimulatory-motif containing DNA hydrogel consisting of polypod-like structured DNA

II-1. Development of nasal antigen delivery system based on immunostimulatory DNA hydrogel for allergy immunotherapy

I developed a controlled release formulation of Cryj1, a major Japanese cedar pollen allergen, with immunostimulatory potency. Two sets of hexapod-like structured DNA (hexapodna) were prepared using six oligodeoxynucleotides (ODNs) with CpG motifs respectively, to obtain an immunostimulatory DNA hydrogel (sDNA hydrogel). A non-immunostimulatory DNA hydrogel (nsDNA hydrogel) was also prepared using ODNs with no CpG motifs. The sDNA hydrogel was more effective than its components or the nsDNA hydrogel for production of interleukin (IL)-12 after addition to murine macrophage-like RAW264.7 cells or after intranasal administration to mice. Then, a Cryj1-loaded sDNA hydrogel (Cryj1/sDNA hydrogel) formulation was prepared by mixing solutions containing both Cryj1 and hexapodna. Cryj1 was slowly released from the sDNA hydrogel in phosphate-buffed saline. After intranasal administration of the fluorescein isothiocyanate (FITC)-labeled Cryj1/sDNA hydrogel in mice, FITC-Cryj1 was retained in the nasal cavity for a longer period than FITC-Cryj1 mixed with hexapodna in solution. Intranasal immunization of mice with the Cryj1/sDNA hydrogel resulted in high levels of Cryj1-specific IgG in nasal lavage fluid (NLF), IL-12 and IFN -γ release from spleen cells after re-stimulation with Cryj1 when compared with intranasal immunization with the other formulations examined. These results indicate that the self-gelling immunostimulatory DNA hydrogel is an effective intranasal formulation for efficient

induction of allergen-specific immune responses.

II- 2. Improvement of sustained release system of antigen from immunostimulatory DNA hydrogel

Chitosan-sDNA hydrogel was obtained by incorporating chitosan, a cationic polymer into sDNA hydrogel. Chitosan-sDNA hydrogel was more stable, showed more solid-like features, had more bound water, and more slowly released FITC-OVA than sDNA hydrogel. Intradermal immunization of mice with the OVA/Chitosan-sDNA hydrogel resulted in induction of high level of OVA-specific IgG in serum compared with OVA/sDNA hydrogel. These results indicate that the sDNA hydrogel mixed with chitosan is an improved formulation for efficient induction of antigen-specific immune responses.

In conclusion, I developed DDS for anticancer agent using plasmid DNA as a carrier and demonstrated its effectiveness for cancer chemo/immunotherapy. Also I demonstrated that immunostimulatory DNA hydrogel was effective as a nasal antigen delivery carrier for allergy immunotherapy. Finally I improved its sustained release property for more effective immunotherapy.

These findings provide evidence that DDS based on CpG DNA is effective for cancer or allergy immunotherapy through simultaneous delivery of immunostimulatory signals and drug or antigen.

Acknowledgements

The author wishes to express sincerely her wholehearted and utmost gratitude to Professor Yoshinobu Takakura for providing me the opportunity to study at Kyoto University, and his considerable understanding, warm support, continuous encouragement, and thoughtful guidance throughout this study.

The author wishes to express her deepest appreciation to Associate Professor Makiya Nishikawa for his patient supervision, insightful comments, suggestions, guidance and direction, valuable discussions and supports facilitating the successful completion of this study throughout the whole this study.

The author would like to express sincere thanks to Assistant Professor Yuki Takahashi for his guidance valuable discussions, advice and supports during the whole this study.

The author would like to express sincere gratitude to Mr. Tomoyuki Naoi for his great achievement and contribution as a co-author for Chapter I, and his advice and warm support for this study.

The author is greatly indebted to Ms. Yuka Umeki and all members of Department of Biopharmaceutics and Drug metabolism and of Drug Delivery Research, Graduate School of Pharmaceutics Sciences, Kyoto University, for their experimental assistance.

The author would like to express gratitude to CMC center of Takeda Pharmaceutical Company LTD. for its warm understanding throughout the course of this study.

Finally, the author would like to express her deepest gratitude to her family for their love, encouragements, support and understanding throughout the course of this study.

List of Publications

Simultaneous delivery of doxorubicin and immunostimulatory CpG motif to tumors using a plasmid DNA/doxorubicin complex in mice.

Yumiko Mizuno, Tomoyuki Naoi, Makiya Nishikawa, Sakulrat Rattanakiat, Nobuko Hamaguchi, Mitsuru Hashida, Yoshinobu Takakura

Journal of Control Release, 2010;141:252-9.

Nasal delivery of Japanese cedar pollen Cryj1 by using self-gelling immunostimulatory DNA for effective induction of immune responses in mice

Yumiko Ishii-Mizuno, Yuka Umeki, Yuki Takahashi, Tetsuji Takabayashi, Shigeharu Fujieda, Yoshinobu Takakura, Makiya Nishikawa

Journal of Control Release, 2015;200:52-9.

Improved sustained release of antigen from immunostimulatory DNA hydrogel by electrostatic interaction with chitosan.

Yumiko Ishii-Mizuno, Yuka Umeki, Yoshinori Onuki, Hiroshi Watanabe, Yuki Takahashi, Yoshinobu Takakura, Makiya Nishikawa

Manuscript in preparation

Other Publication

Biodegradable CpG DNA hydrogels for sustained delivery of doxorubicin and immunostimulatory signals in tumor-bearing mice.

Makiya Nishikawa, Yumiko Mizuno, Kohta Mohri, Nao Matsuoka, Sakulrat Rattanakiat, Yuki Takahashi, Hisakage Funabashi, Dan Luo, Yoshinobu Takakura

Biomaterials, 2011;32:488-494.

References

1. S. Akira, K. Takeda. Toll-like receptor signaling. *Nat. Rev. Immunol.*, 4 (7) (2004), 499–511.
2. P. Ahmad-Nejad, H. Häcker, M. Rutz, S. Bauer, R.M. Vabulas, H. Wagner. Bacterial CpG-DNA and lipopolysaccharides activate Toll-like receptors at distinct cellular compartments. *Eur. J. Immunol*., 32 (7) (2002), 1958–1968.
3. H. Wagner. Interactions between bacterial CpG-DNA and TLR9 bridge innate and adaptive immunity. *Curr Opin Microbiol.*, 5(1) (2002), 62-9.
4. M.M. Whitmore, M.J. DeVeer, A. Edling, R.K. Oates, B. Simons, D. Lindner, B.R. Williams. Synergistic activation of innate immunity by double-stranded RNA and CpG DNA promotes enhanced antitumor activity. *Cancer Res.*, 64 (16) (2004), 5850–5860.
5. D.M. Klinman, A.K. Yi, S.L. Beaucage, J. Conover, A.M. Krieg. CpG motifs present in bacteria DNA rapidly induce lymphocytes to secrete interleukin 6, interleukin 12, and interferon. *Proc Natl Acad Sci USA.*, 93(7) (1996), 2879-83.
6. T. Sparwasser, T. Miethke, G. Lipford, A. Erdmann, H. Häcker, K. Heeg, H. Wagner. Macrophages sense pathogens via DNA motifs: induction of tumor necrosis factor-α-mediated shock. *Eur J Immunol.*, 27 (1997), 1671-9.
7. Y. Kumagai, O. Takeuchi, S. Akira. TLR9 as a key receptor for the recognition of DNA. *Adv Drug Deliv Rev.*, 60 (2008), 795-804.
8. J. Vollmer, A.M. Krieg. Immunotherapeutic applications of CpG oligodeoxynucleotide TLR9 agonists. *Adv Drug Deliv Rev.*, 61 (2009), 195–204.
9. C. Maisonneuve, S. Bertholet, D.J. Philpott, E. De Gregorio. Unleashing the potential of NOD- and Toll-like agonists as vaccine adjuvants. *Proc Natl Acad Sci U S A.*, 111(34) (2014), 12294-9.
10. E.J. Hennessy, A.E. Parker, L.A. O'Neill. Targeting Toll-like receptors: emerging therapeutics? *Nat Rev Drug Discov.*, 9(4) (2010), 293-307.
11. D.E. Fonseca, J.N. Kline. Use of CpG oligonucleotides in treatment of asthma and allergic disease. *Adv Drug Deliv Rev*., 61 (2009), 256–262.
12. A.M. Krieg. Therapeutic potential of Toll-like receptor 9 activation. *Nat Rev Drug Discov.*, 5 (2006), 471-84.
13. A. Trouet, D. Deprez-De Campeneere, C. De Duve Chemotherapy through lysosomes with a DNA–daunorubicin complex. Nat. New Biol., 239 (91) (1972), 110–112.
14. S.H. Um, J.B. Lee, N. Park, S.Y. Kwon, C.C Umbach, D. Luo. Enzyme-catalysed assembly of DNA hydrogel. *Nat Mater.*, 5 (2006), 797-801.
15. M. Nishikawa, K. Ogawa, Y. Umeki, K. Mohri, Y. Kawasaki, H. Watanabe, N. Takahashi, E. Kusuki, R. Takahashi, Y. Takahashi, Y. Takakura. Injectable, self-gelling, biodegradable, and immunomodulatory DNA hydrogel for antigen delivery. *J. Control Release*, 180 (2014) 25–32.
16. F.O. Nestle, S. Alijagic, M. Gilliet, Y. Sun, S. Grabbe, R. Dummer, G. Burg, D. Schadendorf. Vaccination of melanoma patients with peptide- or tumor lysate-pulsed dendritic cells. *Nat. Med.*, 4 (3) (1998), 328–332.
17. S.A. Rosenberg, J.C. Yang, N.P. Restifo. Cancer immunotherapy: moving beyond current vaccines. *Nat. Med.*, 10 (9) (2004), 909–915.
18. E. Gilboa. DC-based cancer vaccines. *J. Clin. Invest.*, 117 (5) (2007), 1195–1203.

19. H. Sezaki, M. Hashida. Macromolecule-drug conjugates in targeted cancer chemotherapy. C*rit. Rev. Ther. Drug Carr. Syst.,* 1 (1) (1984), 1–38.
20. K. Kataoka, G.S. Kwon, M. Yokoyama, T. Okano, Y. Sakurai. Block copolymer micelles as vehicles for drug delivery. *J. Control. Release,* 24 (1–3) (1993), 119–132.
21. A. Gabizon, R. Catane, B. Uziely, B. Kaufman, T. Safra, R. Cohen, F. Martin, A. Huang, Y. Barenholz. Prolonged circulation time and enhanced accumulation in malignant exudates of doxorubicin encapsulated in polyethylene-glycol coated liposomes. *Cancer Res.,* 54 (4) (1994), 987–992.
22. I. Brigger, C. Dubernet, P. Couvreur. Nanoparticles in cancer therapy and diagnosis. *Adv. Drug Deliv. Rev.,* 54 (5) (2002), 631–651.
23. G.P. Adams, L.M. Weiner. Monoclonal antibody therapy of cancer. *Nat. Biotechnol.,* 23 (9) (2005), 1147–1157.
24. H. Maeda, J. Wu, T. Sawa, Y. Matsumura, K. Hori. Tumor vascular permeability and the EPR effect in macromolecular therapeutics: a review. *J. Control. Release,* 65 (1–2) (2000), 271–284.
25. A. Trouet, D. Deprez-de Campeneere, M. de Smedt-Malengreaux, G. Atassi. Experimental leukemia chemotherapy with a "lysosomotropic" adriamycin–DNA complex. *Eur. J. Cancer,* 10 (7) (1974), 405–411.
26. A. Trouet, G. Sokal. Clinical studies with daunorubicin–DNA and adriamycin–DNA complexes: a review. *Cancer Treat. Rep.,* 63 (5) (1979), 895–898.
27. M. Nishikawa, L. Huang. Nonviral vectors in the new millennium: delivery barriers in gene transfer. *Hum. Gene Ther.,* 12 (8) (2001), 861–870.
28. M. Nishikawa, M. Hashida. Nonviral approaches satisfying various requirements for effective in vivo gene therapy. *Biol. Pharm. Bull.,* 25 (3) (2002), 275–283.
29. A.M. Krieg. CpG motifs in bacterial DNA and their immune effects. *Annu. Rev. Immunol.,* 20 (2002), 709–760.
30. T. Yoshinaga, K. Yasuda, Y. Ogawa, Y. Takakura. Efficient uptake and rapid degradation of plasmid DNA by murine dendritic cells via a specific mechanism. *Biochem. Biophys. Res. Commun.,* 299 (3) (2002), 389–394.
31. J.J. Gao, V. Diesl, T. Wittmann, D.C. Morrison, J.L. Ryan, S.N. Vogel, M.T. Follettie. Regulation of gene expression in mouse macrophages stimulated with bacterial CpG-DNA and lipopolysaccharide. *J. Leukoc. Biol.,* 72 (6) (2002), 1234–1245.
32. K. Yasuda, H. Kawano, I. Yamane, Y. Ogawa, T. Yoshinaga, M. Nishikawa, Y. Takakura. Restricted cytokine production from mouse peritoneal macrophages in culture in spite of extensive uptake of plasmid DNA. *Immunology,* 111 (3) (2004), 282–290.
33. T. Yoshinaga, K. Yasuda, Y. Ogawa, M. Nishikawa, Y. Takakura. DNA and its cationic lipid complexes induce CpG motif-dependent activation of murine dendritic cells. *Immunology,* 120 (3) (2007), 295–302.
34. Y. Kuramoto, M. Nishikawa, K. Hyoudou, F. Yamashita, M. Hashida. Inhibition of peritoneal dissemination of tumor cells by single dosing of phosphodiester CpG oligonucleotide/cationic liposome complex. *J. Control. Release,* 115 (2) (2006), 226–233.
35. D.R. Phillips, P.C. Greif, R.C. Boston. Daunomycin–DNA dissociation kinetics. *Mol. Pharmacol.,* 33 (2) (1988), 225–230.
36. K. Kako, M. Nishikawa, H. Yoshida, Y. Takakura. Effects of inflammatory response on in vivo transgene expression by plasmid DNA in mice. *J. Pharm. Sci.,* 97 (8) (2008), 3074–3083.
37. N.R. Bachur, A.L. Moore, J.G. Bernstein, A. Liu. Tissue distribution and disposition of daunomycin

(NCS-82151) in mice: fluorometric and isotopic methods. *Cancer Chemother. Rep.*, 54 (2) (1970), 89–94.
38. K. Kawabata, Y. Takakura, M. Hashida. The fate of plasmid DNA after intravenous injection in mice: involvement of scavenger receptors in its hepatic uptake. *Pharm. Res.*, 12 (6) (1995), 825–830.
39. J. Hisazumi, N. Kobayashi, M. Nishikawa, Y. Takakura. Significant role of liver sinusoidal endothelial cells in hepatic uptake and degradation of naked plasmid DNA after intravenous injection. *Pharm. Res.*, 21 (7) (2004), 1223–1228.
40. K. Wassermann, J. Markovits, C. Jaxel, G. Capranico, K.W. Kohn, Y. Pommier. Effects of morpholinyl doxorubicins, doxorubicin, and actinomycin D on mammalian DNA topoisomerases I and II. *Mol. Pharmacol.*, 38 (1) (1990), 38–45.
41. G. Storm, P.A. Steerenberg, F. Emmen, M. van Borssum Waalkes, D.J. Crommelin DJ. Release of doxorubicin from peritoneal macrophages exposed in vivo to doxorubicin-containing liposomes. *Biochim. Biophys. Acta*, 965 (2–3) (1988), 136–145.
42. R.M. Schiffelers, J.M. Metselaar, M.H. Fens, A.P. Janssen, G. Molema, G. Storm. Liposome-encapsulated prednisolone phosphate inhibits growth of established tumors in mice. *Neoplasia*, 7 (2) (2005), 118–127.
43. T. Ohnuma, J.F. Holland, J.H. Chen. Pharmacological and therapeutic efficacy of daunomycin:DNA complex in mice. *Cancer Res.*, 35 (7) (1975), 1767–1772.
44. Y. Li, Y.D. Tseng, S.Y. Kwon, L. D'Espaux, J.S. Bunch, P.L. McEuen, D. Luo. Controlled assembly of dendrimer-like DNA. *Nat. Mater.*, 3 (1) (2004), 38–42.
45. N.R. Kallenbach, R.I. Ma, N.C. Seeman. *Nature*, 305 (1983) 829 – 831.
46. K. Mohri, M. Nishikawa, Y Takahashi, Y. Takakura. DNA nanotechnology-based development of delivery systems for bioactive compounds. *Eur J Pharm Sci.*, 16 (58) (2014), 26-33.
47. F. Zhang, J. Nangreave, Y. Liu, H. Yan. Structural DNA Nanotechnology: State of the Art and Future Perspective. *J. Am. Chem. Soc.*, *136* (32) (2014), 11198–11211.
48. J. Chao, H. Liu, S. Su, L. Wang, W. Huang, C. Fan. Structural DNA Nanotechnology for Intelligent Drug Delivery. Small, 10(22) (2014), 4626-35.
49. V. Linko, A. Ora, M.A. Kostiainen. DNA Nanostructures as Smart Drug-Delivery Vehicles and Molecular Devices. *Trends Biotechnol.*, 33(10) (2015), 586-94
50. M. Nishikawa, Y. Mizuno, K. Mohri, N. Matsuoka, S. Rattanakiat, Y. Takahashi, H. Funabashi, D. Luo, Y. Takakura. Biodegradable CpG DNA hydrogels for sustained delivery of doxorubicin and immunostimulatory signals in tumor-bearing mice. *Biomaterials*, 32 (2011), 488–94
51. R.K. Viswanathan, W.W. Busse. Allergen Immunotherapy in Allergic Respiratory Diseases. *CHEST,* 141 (2012), 1303–14.
52. G. Scadding, S.R. Durham. Mechanisms of sublingual immunotherapy. *Immunol. Allergy Clin. North Am.*, 31 (2011), 191–209.
53. P.S. Creticos, J.T. Schroeder, R.G. Hamilton, S.L. Balcer-Whaley, A.P. Khattignavong, R. Lindblad, H. Li, R. Coffman, V. Seyfert, J.J. Eiden, D. Broide, the Immune Tolerance Network Group. Immunotherapy with a Ragweed–Toll-Like Receptor 9 Agonist Vaccine for Allergic Rhinitis. *N. Engl. J. Med.* 355 (2006), 1445-55.
54. M.K. Tulic, P.O. Fiset, P. Christodoulopoulos, P. Vaillancourt, M. Desrosiers, F. Lavigne, J. Eiden, Q. Hamid. Amb a 1–immunostimulatory oligodeoxynucleotide conjugate immunotherapy decreases the nasal inflammatory response. *J. Allergy Clin. Immunol.* 113, (2004) 235-41.
55. J.L. Brożek, J. Bousquet, C.E. Baena-Cagnani, S. Bonini, G.W. Canonica, T.B. Casale, R.G. van Wijk,

K. Ohta, T. Zuberbier, H.J. Schünemann, Allergic Rhinitis and its Impact on Asthma (ARIA) guidelines: 2010 Revision. *J. Allergy Clin. Immunol.,* 2010;126:466–76

56. M. Sakashita, T. Hirota, M. Harada, R. Nakamichi, T. Tsunoda, Y. Osawa, A. Kojima, M. Okamoto, D. Suzuki, S. Kubo, Y. Imoto, Y. Nakamura, M. Tamari, S. Fujieda. Prevalence of allergic rhinitis and sensitization to common aeroallergens in a Japanese population, *Int. Arch. Allergy Immunol.,* 151 (2010), 255-61.
57. T. Yamada, H. Saito, S. Fujieda. Present state of Japanese cedar pollinosis: the national affliction. *J. Allergy Clin. Immunol.,* 133 (2014),632-9.e5.
58. M.T. Tse. Oral immunotherapy approved. *Nature Biotechnology*, 32 (2014), 405.
59. Y. Kato, S. Akasaki, Y.M. Haenuki, S. Fujieda, K. Matsushita, T. Yoshimoto. Nasal Sensitization with Ragweed Pollen Induces Local-Allergic-Rhinitis-Like Symptoms in Mice. *PLoS. One,* 9(8) (2014), e103540.
60. J.D.S. Rebouças, I. Esparza, M. Ferrer, M.L. Sanz, J.M. Irache, C. Gamazo. Nanoparticulate Adjuvants and Delivery Systems for Allergen Immunotherapy. *J. Biomed. Biotechnol.,* 2012 (2012), 474605.
61. G. Passalacqua, G.W. Canonica. Local nasal specific immunotherapy for allergic rhinitis. *Allergy Asthma Clin Immunol.,* 15 (2006), 117-23.
62. M. Zaman, S. Chandrudu, I. Toth. Strategies for intranasal delivery of vaccines. *Drug Deliv. and Transl. Res.,* 3 (2013), 100–9
63. M. Suzuki, T. Matsumoto, N. Ohta, W.P. Min, S. Murakami. Intranasal CpG DNA therapy during allergen exposure in allergic rhinitis. *Otolaryngol. Head. Neck Surg.,* 136(2) (2007), 246-51.
64. N. Petrovsky, J.C. Aguilar. Vaccine adjuvants: Current state and future trends. *Immunol. Cell Biol.,* 82(5) (2004) 488-96.
65. T. Nochi, Y. Yuki, H. Takahashi, S. Sawada, M. Mejima, T. Kohda, N. Harada, I.G. Kong, A. Sato, N. Kataoka, D. Tokuhara, S. Kurokawa, Y. Takahashi, H. Tsukada, S. Kozaki, K. Akiyoshi, H. Kiyono. Nanogel antigenic protein-delivery system for adjuvant-free intranasal vaccines. *Nature Materials,* 9, (2010), 572–8.
66. M. Nishikawa, M. Matono, S. Rattanakiat, N. Matsuoka, Y. Takakura. Enhanced immunostimulatory activity of oligodeoxynucleotides by Y-shape formation. *Immunology,* 124 (2008), 247-55.
67. S. Rattanakiat, M. Nishikawa, H. Funabashi, D. Luo, Y. Takakura. The assembly of a short linear natural cytosine-phosphate-guanine DNA into dendritic structures and its effect on immunostimulatory activity. *Biomaterials,* 30 (2009), 5701-6.
68. H. Nazar, M. Roldo, D.G. Fatouros, S.M. van der Merwe, J. Tsibouklis. Hydrogels in Mucosal Delivery. *Therapeutic Delivery,* 3 (2012), 535-55.
69. H. Nazar, D.G. Fatouros, S.M. van der Merwe, N. Bouropoulos, G. Avgouropoulos, J. Tsibouklis , M. Roldo. Thermosensitive hydrogels for nasal drug delivery: The formulation and characterisation of systems based on N-trimethyl chitosan chloride, *Eur. J. Pharm. Biopharm.,* 77 (2011), 225-32.
70. Y. I. Mizuno, Y. Umeki, Y. Takahashi, Y. Kato, T. Takabayashi, S. Fujieda, Y. Takakura, M. Nishikawa. Nasal delivery of Japanese cedar pollen Cryj1 by using self-gelling immunostimulatory DNA for effective induction of immune responses in mice. *J. Control Release,* 200 (2015), 52-9.
71. M.C. Chen, S.F. Huang, K.Y. Lai, M.H. Ling. Fully embeddable chitosan microneedles as a sustained release depot for intradermal vaccination. *Biomaterials,* 34(12) (2013), 3077-86.
72. J.R. Adams, S.L. Haughney, S.K. Mallapragada. Effective polymer adjuvants for sustained delivery of protein subunit vaccines. *Acta. Biomater.,* 14 (2015), 104-14.
73. Y. Umeki, K. Mohri, Y. Kawasaki, H. Watanabe, R. Takahashi, Y. Takahashi, Y. Takakura, M.

Nishikawa. Induction of Potent Antitumor Immunity by Sustained Release of Cationic Antigen from a DNA-Based Hydrogel with Adjuvant Activity. *Adv. Funct. Mater.,* 25 (2015), 5758–5767.

74. E. Celis. Toll-like Receptor Ligands Energize Peptide Vaccines through Multiple Path. *Cancer Res.,* 67(17) (2007), 7945-7.
75. Y. Yang, C.T. Huang, X. Huang, D.M. Pardoll. Persistent Toll-like receptor signals are required for reversal of regulatory T cell–mediated CD8 tolerance. *Nat Immunol.,* 5(5) (2004), 508-15.
76. C.M. Jewell, S.C. López, D.J. Irvine. In situ engineering of the lymph node microenvironment via intranodal injection of adjuvant-releasing polymer particles. *Proc. Natl. Acad. Sci. U S A,* 108(38) (2011), 15745-50.
77. N. Bhattarai, J. Gunn, M. Zhang. Chitosan-based hydrogels for controlled, localized drug delivery. *Adv. Drug Deliv. Rev.,* 62(1) (2010), 83-99.
78. S.A. Agnihotri, M.N. Mallikarjuna, T.M. Aminabhavi. Recent advances on chitosan-based micro- and nanoparticles in drug delivery. *J. Control. Release,* 100(1) (2004), 5-28.
79. H.Q.Mao, K. Roy, V.L. Troung-Le, K.A. Janes, K.Y. Lin, Y. Wang, J.T. August, K.W. Leong. Chitosan-DNA nanoparticles as gene carriers: synthesis, characterization and transfection efficiency. *J. Control. Release,* 70(3), (2001), 399-421.
80. A. Chenite, C. Chaput, D. Wang, C. Combes, M.D. Buschmann, C.D. Hoemann, J.C. Leroux, B.L. Atkinson, F. Binette, A. Selmani. Novel injectable neutral solutions of chitosan form biodegradable gels in situ. *Biomaterials,* 21(21) (2000), 2155-61.
81. G. Molinaro, J.C. Leroux, J. Damas, A. Adam. Biocompatibility of thermosensitive chitosan-based hydrogels: An in vivo experimental approach to injectable biomaterials. *Biomaterials,* 23(13) (2002), 2717-22.
82. Y. Onuki, N. Hasegawa, C. Kida, Y. Obata, K. Takayama. Study of the contribution of the state of water to the gel properties of a photocrosslinked polyacrylic acid hydrogel using magnetic resonance imaging. *J. Pharm. Sci.,* 103(11) (2014), 3532-41.
83. X. Guan, M. Nishikawa, S. Takemoto, Y. Ohno, T. Yata, Y. Takakura. Injection site-dependent induction of immune response by DNA vaccine: comparison of skin and spleen as a target for vaccination. *J. Gene. Med.,* 12(3) (2010), 301-9.
84. P. He, S.S. Davis, L. Illum. Sustained release chitosan microspheres prepared by novel spray drying methods. *J. Microencapsul.,* 16(3) (1999), 343-55.
85. S. Mansouri, P. Lavigne, K. Corsi, M. Benderdour, E. Beaumont, J.C. Fernandes. Chitosan-DNA nanoparticles as non-viral vectors in gene therapy: strategies to improve transfection efficacy. *Eur J Pharm Biopharm.* 57(1) (2004), 1-8.
86. S. Ozawa, A. Mirelman, M.L. Stack, D.G. Walker, O.S. Levine.Cost-effectiveness and economic benefits of vaccines in low- and middle-income countries: a systematic review. *Vaccine,* 31(1) (2012), 96-108.
87. Y. Mizuno, T. Naoi, M. Nishikawa, S. Rattanakiat, N. Hamaguchi, M. Hashida, Y. Takakura. Simultaneous delivery of doxorubicin and immunostimulatory CpG motif to tumors using a plasmid DNA/doxorubicin complex in mice. *J. Control. Release,* 141(2) (2010), 252-9.